Impact of Increased Penetration of DFIG Based Wind Turbine Generators on Rotor Angle Stability of Power Systems

by

Durga Gautam

A Dissertation Presented in Partial Fulfillment
of the Requirements for the Degree
Doctor of Philosophy

Approved November 2010 by the
Graduate Supervisory Committee:

Vijay Vittal, Chair
Gerald Heydt
Raja Ayyanar
Richard Farmer
Jennie Si

ARIZONA STATE UNIVERSITY

December 2010

ABSTRACT

An advantage of doubly fed induction generators (DFIGs) as compared to conventional fixed speed wind turbine generators is higher efficiency. This higher efficiency is achieved due to the ability of the DFIG to operate near its optimal turbine efficiency over a wider range of wind speeds through variable speed operation. This is achieved through the application of a back-to-back converter that tightly controls the rotor current and allows for asynchronous operation. In doing so, however, the power electronic converter effectively decouples the inertia of the turbine from the system. Hence, with the increase in penetration of DFIG based wind farms, the effective inertia of the system will be reduced.

With this assertion, the present study is aimed at identifying the systematic approach to pinpoint the impact of increased penetration of DFIGs on a large realistic system. The techniques proposed in this work are tested on a large test system representing the Midwestern portion of the U.S. Interconnection. The electromechanical modes that are both detrimentally and beneficially affected by the change in inertia are identified. The combination of small-signal stability analysis coupled with the large disturbance analysis of exciting the mode identified is found to provide a detailed picture of the impact on the system. The work is extended to develop suitable control strategies to mitigate the impact of significant DFIG penetration on a large power system.

Supplementary control is developed for the DFIG power converters such that the effective inertia contributed by these wind generators to the system is increased. Results obtained on the large realistic power system indicate that the fre-

quency nadir following a large power impact is effectively improved with the proposed control strategy. The proposed control is also validated against sudden wind speed changes in the form of wind gusts and wind ramps. The beneficial impact in terms of damping power system oscillations is observed, which is validated by eigenvalue analysis.

Another control mechanism is developed aiming at designing the power system stabilizer (PSS) for a DFIG similar to the PSS of synchronous machines. Although both the supplementary control strategies serve the purpose of improving the damping of the mode with detrimental impact, better damping performance is observed when the DFIG is equipped with both the controllers.

ACKNOWLEDGEMENTS

I would like to express my sincere gratitude and profound respect to my advisor Dr. Vijay Vittal, for giving me the opportunity to work with him in this very interesting area and for his worthwhile suggestions and encouragement. His unreserved willingness to spare precious time on guidance, feedback and advice are the major element to make this work a successful completion.

I would like to express my sincere respect and gratitude to my dissertation committee members, Dr. Gerald Heydt, Dr. Raja Ayyanar, Professor Richard Farmer and Dr. Jennie Si for their constructive comments and guidance.

I would also like to take this opportunity to thank the National Science Foundation and the Power System Engineering Research Centre for sponsorship of this research.

My special thanks goes to all the friends and well wishers who contributed by ways and means.

I feel a deep sense of gratitude for my mother and my late father for being continuous source of motivation and inspiration throughout my life. I owe a debt of gratitude to my beloved husband, Bishnu, for his love, support and encouragement when I needed the most. I am deeply indebted to my brother Kailash and my sister Deepa for their love and understanding. It is to my family and their love that this work is dedicated.

TABLE OF CONTENTS

Page

CHAPTER Page

LIST OF TABLES

LIST OF FIGURES

Figure Page

NOMENCLATURE

$\boldsymbol{A}$	state or plant matrix
A_r	area swept by the rotor blades
$\boldsymbol{B}$	input matrix
$\boldsymbol{C}$	output matrix
C_p	power coefficient
$\boldsymbol{D}$	feed forward matrix
DFIG	doubly fed induction generator
f	frequency of oscillation
FCWTG	full converter wind turbine generator
G	gain of the supplementary control loop
$\boldsymbol{g}$	matrix of system algebraic equations
GE	General Electric
GENROU	round rotor generator model
GWEC	global wind energy council
H	inertia constant
$\boldsymbol{h}$	matrix of system non linear equations
$\boldsymbol{I}$	identity matrix
I_p	active current command to the DFIG converter
I_{pmax}	short term active current capability of the DFIG converter
J	moment of inertia
K_b	equivalent wind turbine radius coefficient
P_e	electrical power output of the generator

p_{ji}	participation factor of the j^{th} variable in the i^{th} mode
P_m	mechanical power extracted from the wind
P_{max}	maximum active power order
P_{ord}	active power order
P_r	power delivered to the rotor
P_s	power delivered by the stator
PSAT	power flow and short circuit analysis tool
PSS	power system stabilizer
Q_{max}	maximum reactive power limit of DFIG unit
Q_{min}	minimum reactive power limit of DFIG unit
s	slip
$S_{B,sys}$	system MVA base
S_{BM}	rated MVA of DFIG wind farm
SMIB	single machine infinite bus
SSAT	small signal analysis tool
T_e	generator electrical torque
T_m	generator mechanical torque
TSAT	transient security assessment tool
T_{set}	DFIG torque set point
TSI	transient stability index
TSR	ratio of the rotor blade tip speed and wind speed
$\boldsymbol{u}$	input matrix
$\boldsymbol{v_i}$	right eigenvector

v_{ji}	j^{th} entry of the right eigenvector $\boldsymbol{v_i}$
V_t	DFIG terminal voltage
v_w	wind speed
$\boldsymbol{w_i}$	left eigenvector
w_{ij}	j^{th} entry of the left eigenvector $\boldsymbol{w_i}$
WTG	wind turbine generator
$\boldsymbol{x}$	state variable matrix
x_j	j^{th} state variable
$\boldsymbol{y}$	output matrix
α	generator angular acceleration
δ_{max}	maximum angle separation of two generators
ξ	damping ratio
η	transient stability index
θ	blade pitch angle
λ	eigenvalue
ρ	air density
σ	real part of complex eigenvalue
$\Delta\omega_{max}$	maximum deviation in grid frequency
ω	imaginary part of complex eigenvalue
ω_e	generator rotor speed
ω_{err}	speed error
ω_{grid}	grid frequency
ω_{nominal}	nominal grid frequency

ω_{ref}	reference rotor speed
ω_t	rotational speed of the turbine

CHAPTER 1

INTRODUCTION

1.1 Background

The emergent pace of wind energy projects in various countries around the world has put wind energy at the forefront of the energy destiny. Among the various renewable energy resources, wind power is assumed to have the most favorable technical and economical prospects [1].

Several countries are taking steps to develop large-scale wind markets. According to news released by the Global Wind Energy Council (GWEC), the sum of the world's total wind installations increased by 31% to reach over 157.9 GW by the end of 2009 [2]. The increase in capacity of over 100% from 12.1 GW in 2008 to 25.1 GW (with new capacity additions of 13 GW) by the end of 2009 made China the number one market the in terms of new wind power installations. The United States installed nearly 10 GW of wind power in 2009 increasing the nation's installed capacity by 39% and bringing the total capacity to 35 GW. Maintaining the record of the year 2008, United States remains the leading nation in wind power in the year 2009 with 22.3% of world total installed wind capacity. Following in rank are China, Germany, and Spain with installed capacities of 25.80 GW, 25.77 GW and 19.14 GW respectively.

The wind turbine generators (WTGs) in a wind farm are distributed within the farm, but the total output of the farm normally connects to the bulk power system at a single substation, in a fashion similar to conventional central-station gen-

eration [3]. There are many different generator types for wind-power applications in use today. Among the several wind generation technologies, variable speed wind turbines utilizing doubly fed induction generators (DFIGs) are gaining momentum in the power industry due to their improved efficiency and controllability. The higher efficiency is achieved due to the ability of the DFIG to operate near its optimal turbine efficiency over a wider range of wind speeds through variable speed operation. This is achieved through the application of a back-to-back converter that tightly controls the rotor current and allows for asynchronous operation. Consequently, the power system originally designed for conventional synchronous generation experiences change in dynamics and operating characteristics.

System stability and dynamics can be evaluated by observing the behavior of the system when subjected to a disturbance. A stable power system is one in which the system dominant with synchronous machines when perturbed, will either return to their original state if there is no net change of power or will acquire a new state without losing synchronism [4]. The perturbations can be of several types and can lead to two major categories of rotor angle instabilities, namely, transient instability and small signal instability. Usually, the small perturbation causes a transient that is oscillatory in nature and if the system is stable, oscillations will be damped. Large perturbations such as three phase short circuit faults, on the other hand, may result in transients that instigate aperiodic angular separation of the generator rotors.

1.2 Problem statement and rationale

The penetration of power electronic based variable speed wind turbine generators such as DFIGs shows marked impact on stability of the system. Following a large disturbance, the restoring forces that bring the position of the affected generators back to nominal values are related to the interaction between the synchronizing forces and the total system inertia. In the case of DFIGs, however, the electrical power generated by the unit is effectively tightly controlled by the current control loops of the converter. Thus, following an electrical disturbance the converter quickly controls the DFIG unit to return to the unit's pre-disturbance power output, thereby effectively decoupling the potential inertial response of the turbine from the system. Thus, with the increased penetration of these DFIG based wind farms, the effective inertia of the system will be reduced.

The impact of the reduced inertia is twofold: (i) following a disturbance the effective aggregated angular acceleration of synchronous generators would be increased and as a result the restoring forces would have to be larger to bring the disturbed machines back to equilibrium position, and (ii) the rate of frequency decay and thus the nadir of frequency decline would be increased for loss of generation events. Consequently, the transient stability performance of the system could be lowered for certain disturbances.

The converter decouples the turbine from the grid by not only controlling the rotor speed and electrical power, but also damping out any rotor speed oscillations that may occur within the WTG. DFIGs primarily only have four mechan-

isms by which they can affect the damping of electromechanical modes (since they themselves do not participate in the modes):

1. Displacing synchronous machines thereby affecting the modes
2. Impacting major path flows thereby affecting the synchronizing forces
3. Displacing synchronous machines that have power system stabilizers
4. DFIG controls interacting with the damping torque on nearby large synchronous generators

Furthermore, the changes in operational structure due to the placement of wind farms can impact the oscillations. Wind farms are normally located far from major load centers. This constitutes power transfer over longer distances and might involve power flow through congested lines. This scenario might lead to significant change in generation profile and power flow, consequently, affecting the small signal stability of the system. Given this premise, the initial part of the present work encompasses the issues related to system dynamic performance with the penetration of DFIG wind farms. The impact study is carried out by perturbing the system with short circuit faults and applying disturbances at various locations in the system.

The inertia constants of conventional synchronous generators of a large power plant are in the order of 2-9 s [5] and this inertia is automatically available as the frequency of the grid tends to decrease following a disturbance or loss of generation/transmission line. In the case of DFIGs, as discussed above, the inertia of the turbine is effectively decoupled from the system. The decoupling of the in-

ertia in DFIGs, however, can be overcome by appropriate use of control. Significant amount of kinetic energy is stored in the rotating turbine blades with typical inertia constants in the range of 2-6 s [6]. It is possible to exploit the isolated inertia and support the system if proper control mechanisms are developed.

The primary input in the case of DFIGs, the wind flow, cannot be changed. Yet, the kinetic energy stored in the rotating masses of a wind turbine can be exploited to provide primary frequency control for short time periods. In this framework, the objectives of the proposed work are outlined in the following section.

1.3 Objectives

The overall objective of this research is to study and mitigate the impact of increased penetration of DFIG based WTGs on transient and small signal stability of the system. The transient stability as well as electromechanical damping performance of the system would be assessed for various specific objectives as follows:

- To observe the system dynamic performance when DFIG based wind farms are added to the system with a concomitant decrease in conventional generators
- To analyze the distinct correlation between the types of disturbance, location of disturbance and operating condition with reference to the increased wind penetration that affects system stability.

- To develop control strategies to mitigate the impact of reduced inertia due to increased DFIG penetration.
- To develop a supplementary control strategy for damping power oscillations

1.4 Dissertation organization

The dissertation is organized in seven chapters. Chapter 1 covers an introduction which presents the background of the study. The chapter contains the problem statement and rationale and objectives of the study.

Chapter 2 presents the review of literature with regard to several commercially available wind generator technologies. The chapter further includes review of related works being carried out with regard to modeling and control of DFIG and its impact on power system stability.

Chapter 3 discusses on modeling and control of DFIG based wind turbines so as to provide frequency support and to improve overall system stability.

Chapter 4 deals with the impacts of wind power penetration on power system stability. The chapter details the fundamental concepts and provides definitions of small signal stability and transient stability. The chapter further relates the frequency control mechanism of conventional synchronous generators to that of DFIG based wind farms and explores the effect of overall system inertia.

Chapter 5 sets out the approach used to study the impact of increased penetration of DFIG on a large test system. The chapter includes a formulation whereby the DFIG based wind farms mimic the inertia of synchronous generators.

The underlying assumptions, tools, software and test system used in the analysis has been described in this chapter.

In Chapter 6 the simulation results and inferences drawn are presented. Several cases have been considered to depict possible scenarios and results have been shown in graphical and tabular format. The general and specific conclusions that can be drawn from the analyses are presented in appropriate fashion.

Chapter 7 concludes the work carried out so far by summarizing the important results and giving emphasis to the new contributions of the dissertation.

CHAPTER 2

LITERATURE REVIEW

Numerous research efforts have been devoted to address the challenges raised by the proliferation of wind power. This chapter presents the review of literature concerning the modeling of wind turbines, the effect that increased wind power penetration can have on power systems, and the control strategies to mitigate the impact due to the DFIG wind farms. The optimal integration of these wind farms can only be achieved when the changed scenario does not jeopardize the system stability during normal operation as well as during network disturbances. Given this premise, the effect of wind power penetration on the power system stability is reviewed with special focus on transient and small signal stability. Several control mechanisms proposed in the literature with regard to mitigating the impact of DFIG penetration are discussed.

The most common types of wind generators for large scale wind power applications are the self excited induction generators and doubly fed induction generators [1]. There are many different generator types for wind power applications in use today. The main distinction can be made between fixed speed and variable speed wind generator types. Three most common types of wind turbine concepts, namely, squirrel cage induction generator, doubly fed induction generator (DFIG) and full converter wind turbine generator (FCWTG) have been widely reported in literatures[7].

2.1 Fixed speed wind turbine generator

In the early stages of wind power development, most wind farms were equipped with fixed speed wind turbines and induction generators. A fixed speed wind generator is usually equipped with a squirrel cage induction generator whose speed variations are limited. Normally, pitch controllers are incorporated in variable speed turbine. However, fixed speed turbines can also be augmented with a pitch controller. In doing so, the mechanical power output from the turbine can be varied even for fixed rotor speed.

Because the efficiency of wind turbines depends on the tip-speed ratio, the power of a fixed speed wind generator varies directly with the wind speed [8]. Since induction machines have no reactive power control capabilities, fixed or variable power factor correction systems are usually required for compensating the reactive power demand of the generator. Figure 2.1 shows the schematic diagram of the fixed speed induction machine.

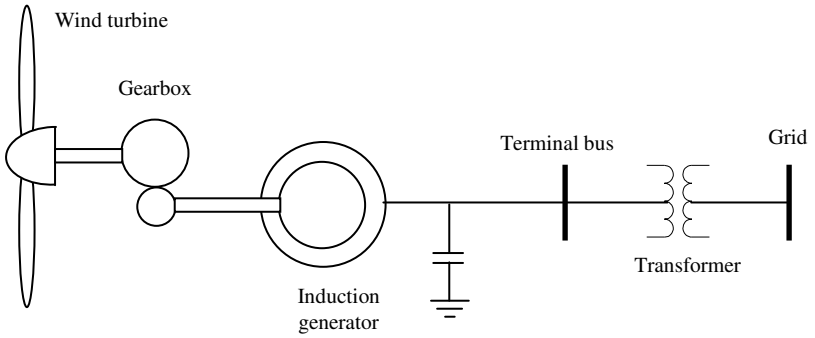

Figure 2.1 Fixed speed wind turbine generator

2.2 Variable speed wind turbine generator

Several technologies and historical applications of variable speed wind generator have been discussed in [9]. Variable speed concepts allow operating the wind turbine at the optimum tip-speed ratio and hence at the optimum power coefficient for a wide wind speed range. The variable speed configuration is very flexible, in that it can be used to control different parameters, namely, active and reactive power, torque, power factor or terminal voltage. The variable speed WTGs can act as a reactive power source or supply in contrast to a fixed speed generator which always absorbs reactive power. The two most widely used variable speed wind generator concepts are the DFIG and the full converter wind turbine (FCWTG).

2.2.1. Doubly fed induction generator wind turbine

Due to advantages such as high energy efficiency and controllability, the variable speed wind turbine using DFIG is getting more attention. A DFIG is basically a standard, wound rotor induction generator with a voltage source converter connected to the slip-rings of the rotor. The stator winding is coupled directly to the grid and the rotor winding is connected to a power converter as shown in Figure 2.2.

The converter system enables two way transfer of power. The grid side converter provides a dc supply to the rotor side converter that produces a variable frequency three phase supply to the generator rotor via slip rings. The variable voltage into the rotor at slip frequency enables variable speed operation. Manipu-

lation of the rotor voltage permits the control of the generator operating conditions.

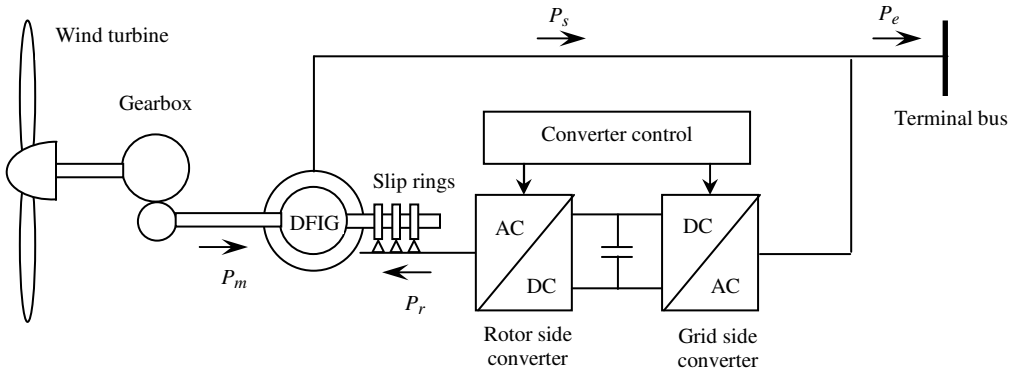

Figure 2.2 Doubly fed induction generator

In case of low wind speeds, the drop in rotor speed may lead the generator into a sub-synchronous operating mode. During this mode, the DFIG rotor absorbs power from the grid. On the other hand, during high wind speed, the DFIG wind turbine running at super synchronous speed will deliver power from the rotor through the converters to the network. Hence, the rotational speed of the DFIG determines whether the power is delivered to the grid through the stator only or through the stator and rotor [10]. The power delivered by the rotor and stator is given by [11],

$$P_r = sP_s \tag{2.1}$$

$$P_e = (1 \pm s)P_s \tag{2.2}$$

where, P_e is the electrical power output of the generator, P_s is the power delivered by the stator and P_r is the power delivered to the rotor.

However, under all operating situations, the frequency of rotor supply is controlled so that under steady conditions, the combined speed of the rotor plus the rotational speed of the rotor flux vector matches that of the synchronously rotating stator flux vector fixed by the network frequency [16]. Hence, the power could be supplied to the grid through the stator in all three the modes of operation, namely, sub synchronous, synchronous and super synchronous modes. This provides the DFIG a unique feature beyond the conventional induction generator as the latter can deliver power to the grid during super synchronous speed only.

2.2.2. Full converter wind turbine generator

This category of wind turbine uses a synchronous generator that can either be an electrically excited synchronous generator or a permanent magnet machine. To enable variable-speed operation, the synchronous generator is connected to the network through a variable frequency converter, which completely decouples the generator from the network. The electrical frequency of the generator may vary as the wind speed changes, while the network frequency remains unchanged. The rating of the power converter in this wind turbine corresponds to the rated power of the generator plus losses. The schematic of the converter driven synchronous generator based wind turbine is as shown in Figure 2.3.

Due to the improved efficiency of energy transfer from the wind and reduced mechanical stresses, many large wind turbines operate at variable speed using DFIGs. The DFIG has become the most widely used generator type for units above 1 MW [12].

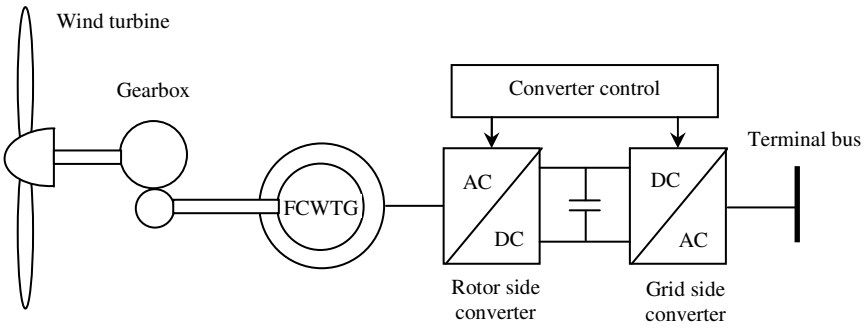

Figure 2.3 Full converter wind turbine generator

The unpredictability inherent with the wind resource makes it difficult to predict the power production in advance. As the wind power penetration increases, there would be substantial share of variable power generation. The provision of generation reserve and frequency control thus becomes an important issue [13]. Moreover, if the wind farms connected to the bulk transmission system were to trip in response to grid disturbances, then the total loss of generation would increase. This also necessitates increased level of spinning reserve in order to make the system secure [14,15]. On the other hand, if the wind penetration is high enough to displace the central generating plant, the ancillary services have to be provided by some others means. The associated additional cost will thus ultimately reduce the value of wind power [13]. Without a solution to these problems, wind power cannot compete as a primary source of electricity.

A control scheme for DFIGs with some important capabilities, namely, voltage support following network faults, power system stabilizer capability that improves system damping and short-term frequency support following loss of network generation has been proposed in [16]. The paper advocates that the pro-

posed control scheme can withstand significantly longer fault clearance times for three phase faults than a synchronous generator with conventional excitation control. Reference [17] proposes an approach wherein the DFIG wind farms can actively provide primary reserve for frequency control. The paper exemplifies that DFIG wind farms equipped with the speed-droop control mechanism can provide spinning reserve that could be made available as an ancillary service. However, in order to provide primary response reserve, DFIG wind farms should be operated below the maximum wind extraction curves. A control scheme to improve the frequency response of a full converter variable speed wind turbine generator with permanent magnet synchronous generator is proposed in [18]. The paper compares the frequency control capability of the wind turbine with that of conventional synchronous generator and advocates that the full converter wind turbine has the advantage of flexibly controlling its active power output. A methodology to improve system temporary minimum frequency in a hydro dominated system has been proposed in [19]. The rotational energy of turbine blades of the variable speed wind turbine has been deployed to provide short term extra active power support. The paper illustrates a condition wherein the support from wind turbine is equivalent to the support of a conventional synchronous machine with 1.8 s inertia constant.

With wide spread deployment in the electrical network, DFIG units are required to satisfy challenging grid codes. Accurate control and modeling of the units, thus, becomes a primary factor. Several research efforts have dealt with the

control and modeling of these wind turbines. A single cage and double cage representation of the rotor together with the control and protection circuits has been proposed in [20]. The model proposed in the paper is simulated for various system disturbances so as to observe the behavior of the network and the wind farm. The paper concludes that stability of DFIG can be enhanced with the proper selection of proportional gain of the speed and power factor controller. The comparative study of several subsystems used in DFIG models with special reference to their transient responses is carried out in [21]. The paper addresses model parameters and simplifications associated with aerodynamic rotor, shaft dynamics, machine model and converter representation. The paper however advocates that the shaft stiffness plays a major role in shaft dynamics and can result in active power oscillations thus influencing the transient recovery of DFIGs. According to [22], the DFIG equipped with four-quadrant ac-to-ac converter increases the transient stability margin of the electrical grids compared to the fixed speed wind systems based on cage generators. The effect of integration of DFIGs on transient stability of a weak transmission system is covered in [23]. The paper concludes that the DFIGs equipped with power electronics converters and fault ride through capability will have no adverse effect on the stability of an electrically weak grid. The transient stability of grid connected DFIGs for an external short circuit fault is analysed in [24]. When the short circuit fault leads to very low terminal voltage, the protection system and control strategy proposed in the paper restores the voltage and ensures the normal operation of the wind turbine after the fault clearance.

Reference [25] focuses on the operational mode of variable speed wind turbines that could enhance the transient stability of nearby conventional generators.

Power system oscillations occur due to the lack of damping torque. The oscillation of power system variables (bus voltage, bus frequency, active and reactive powers, etc.) is caused due to the oscillation of generator rotor [26]. Several research efforts have dealt with the impact of large scale wind power penetration on power system oscillations. The effect of wind farms on the modes of oscillation of a two-area, four-generator power system has been analyzed in [27]. The paper focuses on the model characteristics of the system with the integration of wind farms. Reference [28] advocates that the generator types used in wind turbines do not take part in power system oscillations. Rather, the penetration of wind power will have a damping effect due to reduction in the size of synchronous generators that engage in power system oscillations. The paper concludes that constant speed wind turbines damp power oscillations better than variable speed turbines. On the other hand, reference [29] advocates that adequately controlled variable speed wind farms based on DFIGs can improve the frequency dynamics. A small signal model based on the detailed model of the DFIG and its associated control is derived in [30]. The paper advocates that controller parameters have significant effect on the stability of power systems, while the latter can be improved with the proper set of control parameters. Among several optimization methods, particle swarm optimization method has been proposed in [31] to optimize of the controller parameters. The paper states that the fault ride-through capabili-

ty of DFIG can also be improved using the optimized controller. The effect of wind power integration on power system oscillations under varying operating conditions is dealt with in [32]. The paper concludes that with increased wind power, damping is reduced which is accompanied by congestion at weak interconnection lines. The eigenvalue analysis of a single machine infinite bus (SMIB) with respect to the change in system parameters, operating condition and grid strength is carried out in [33].

Mechanisms to supplement DFIGs with frequency response capability have drawn considerable research interest recently. An approach to introduce inertial response in variable speed wind turbines is proposed in [34]. The technique is based on changing the DFIG torque set point based on the derivative of system frequency. This technique, however, has limitations. Firstly, being an improper transfer function, the derivative function can only be approximated. Secondly, the derivative block has high gain for high frequency signals and as a result is very susceptible to noise signals. The work carried out in [35] advocates a similar approach and proposes a supplementary control which provides a response akin to the natural inertial response. Primary frequency control based on deviation of grid frequency is proposed in [36]. A similar concept together with a scheme to provide frequency response by de-loading the wind turbine is proposed in [37,38]. This mechanism is beneficial when the system has frequent load generation imbalances and wind turbines are required to provide the support accordingly. Unless required to do so, de-loading is undesirable as it reduces the efficiency of ex-

ploiting aerodynamic power, the main incentive for DFIG application. The work carried out in [39] puts some figures on the peak and duration of maximum active power that can be extracted for a commercially available GE 3.6 MW wind turbine. The work also addresses the possibility of varying the wind turbine physical parameters as well. The control concept presented in [40] aims to provide an incremental energy equivalent to a synchronous generator with an inertia constant of 3.5 MWs/MVA. The concept is validated in a hydro dominated system where the support is provided for first 10secs of grid event. Reference [41] advocates that asynchronous coupling of WTG permits generator speed drops up to 0.7 p.u., which considerably increases its kinetic energy discharge capability compared to conventional plants. According to [42] wind turbine frequency response is limited to a short period. The paper proposes the idea of coordination with conventional generation units by feeding additional signal based on participation factors.

In order to improve the system damping with the high penetration of DFIG based wind farms, the concept of auxiliary PSS loop for DFIG has been introduced in the literature recently. The auxiliary PSS loop proposed in [43] is believed to change the stator currents of DFIGs so as to increase the damping torques of the synchronous generators in the system. The control philosophy adopted in the paper is similar to the PSS of the synchronous generators and consists of a washout block, PSS gain and phase compensation while the input signal is derived from the DFIG stator electrical power. An auxiliary signal derived from the frequency deviation is used as the input to the PSS in [44]. For the test system

considered in the paper, interarea oscillation damping is found to improve with the proposed PSS. The supplementary control signal derived from the terminal voltage is used as the input to the PSS in [45]. The stabilizing signal is fed to the rotor quadrature voltage in the active power control loop so as to provide additional damping.

CHAPTER 3

MODELING AND CONTROL OF DOUBLY FED INDUCTION GENERATOR

The modeling of DFIGs can be classified into two broad categories, namely, modeling for steady state analysis and for dynamic analysis [46].

3.1 Modeling for steady state analysis

Although the wind turbines are distributed within the wind farm, the bulk power from the latter is connected to the grid at a single substation. Consequently, WTGs within the farm are aggregated into a single unit having an MVA rating equal to the summation of the MVA rating of the individual units. Furthermore, as DFIG units have reactive power capability, the wind farm is modeled in a manner similar to the conventional generator for steady state analysis and is represented as a PV bus with appropriate VAr limits [47]. The modeling of a GE WTG represented by a single model, with a simplified representation of the collector system is shown in Figure 3.1 [46].

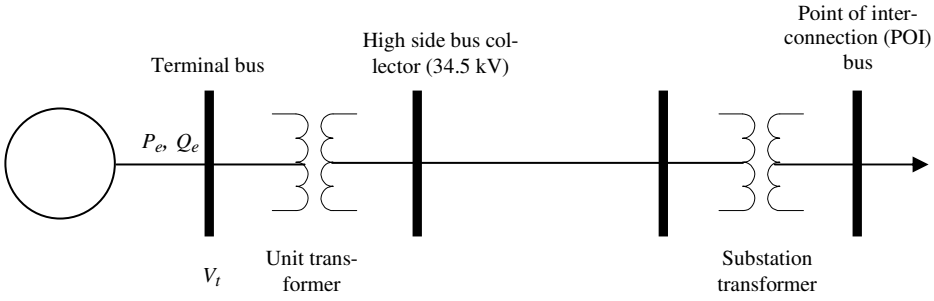

Figure 3.1 Power flow model of wind farm [46]

3.2 Modeling for dynamic analysis

The power flow provides initial conditions for dynamic simulation. For power system dynamic simulations, the wind farm is modeled as a single equiva-

lent machine as shown in Figure 3.1. A complete model of the wind farm with large number of wind turbines will increase the computational burden. The aggregated model is applicable when the purpose is to observe the influence of disturbances and other impact on the power network rather than within the wind farm [29]. Several components that contribute to the dynamic behavior of a DFIG are outlined as follows and included in the analysis conducted [47],

- Turbine aerodynamics
- Turbine mechanical control (also called pitch control) that controls the mechanical power delivered to the shaft
- Shaft dynamics modeled as a two mass shaft, one mass represents rotor/turbine blades and the second represents the generator
- Generator electrical characteristics – as the rotor side converter drives the rotor current very fast, the rotor flux dynamics is neglected and the model behaves as a controlled current source
- Electrical controls - three controllers are used to provide controls for frequency/active power, voltage/reactive power, and pitch angle/mechanical power
- Protection relay settings

Figure 3.2 shows the overall components of a WTG model.

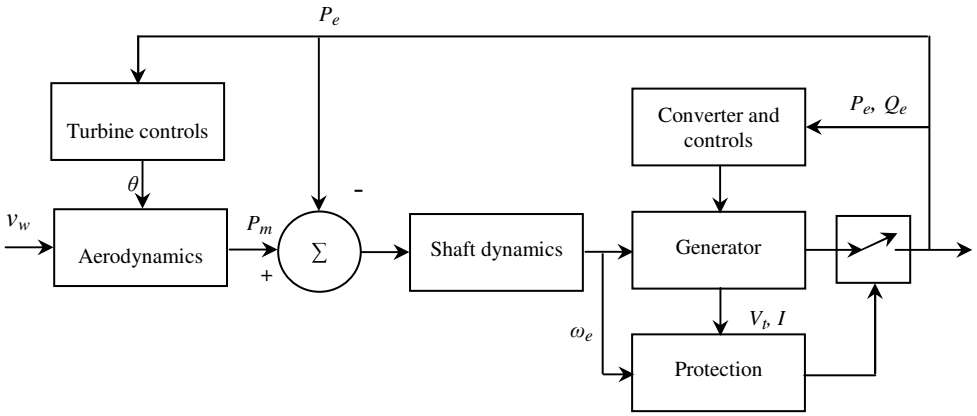

Figure 3.2 Components of a WTG model [47]

Although the parameters for the aerodynamics, turbine controls and protection systems for the various types of WTG might be different from one manufacturer to another, the model structure will essentially be similar. In the case of stall controlled units, there is no turbine blade pitch control. For constant speed units, blade pitch will be used to regulate power instead of speed on variable-speed units.

3.3 DFIG control models

The DFIG model used throughout this work is based on the GE 1.5 MW model documented in [12,13]. Three main controllers provide controls for frequency/active power, voltage/reactive power, and pitch angle/mechanical power. The output of these three controllers would be the input to the end block of the DFIG which is essentially the wind generator model. The operating condition of the generator in the power flow is used to initialize the model and the outputs from the model are the current injections into the network at the generator bus.

Additionally, a model implemented to calculate the reference rotor speed (ω_{ref}) based on the electric power output (P_e) is also considered. The normal value of the reference rotor speed is 1.2 p.u. at rated wind speed, but for power output levels below 75%, the reference speed is evaluated as follows [13],

$$\omega_{ref} = -0.67P_e^2 + 1.42P_e + 0.51. \tag{3.1}$$

The schematic diagram of the DFIG active power and pitch angle controllers is shown in Figure 3.3. The turbine aerodynamics is associated with the extraction of mechanical power from the wind for a given pitch angle and tip speed ratio (ratio of rotational speed of turbine to the wind speed). The wind power model computes the mechanical power extracted from the wind as follows [12],

$$P_m = \frac{\rho}{2} A_r v_w^3 C_p(TSR, \theta) \tag{3.2}$$

where, P_m is the mechanical power extracted from the wind, ρ is the air density, A_r is the area swept by the rotor blades, v_w is the wind speed, C_p is the power coefficient, TSR is the tip speed ratio and θ is the blade pitch angle. The tip speed ratio can be calculated as [46],

$$TSR = K_b \frac{\omega_t}{v_w} \tag{3.3}$$

where, ω_t is the rotational speed of the turbine and K_b is equivalent wind turbine radius coefficient.

As shown in Figure 3.3 the inputs to the wind power model are wind speed (v_w), pitch angle (θ) and turbine angular speed (ω_t). The mechanical power extracted is controlled by the pitch angle controller. For wind speeds beyond rated value, blades are pitched to limit the mechanical power delivered to the shaft to

the equipment rating (1.0 p.u.). When the wind speed is less than the rated value, blades are set at minimum pitch to maximize the mechanical power.

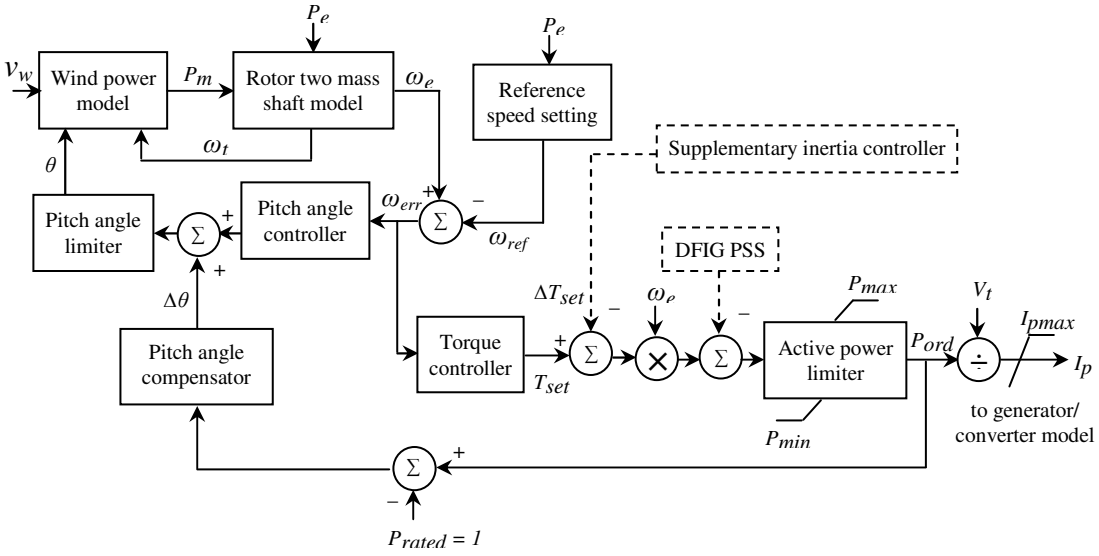

Figure 3.3 Schematic diagram showing active power and pitch angle controllers of DFIG

The mechanical power evaluated by the wind power model and electrical power injected to the grid is used to solve the induction generator equation of motion. The shaft dynamics is modeled as two masses taking into account separate masses for the turbine blades and the electrical generator. The model thus evaluates the generator rotor speed (ω_e) and turbine speed (ω_t). The deviation of rotor speed from the reference (ω_{ref}) actuates the pitch angle controller and torque control module simultaneously.

In addition to actuating the pitch angle controller in response to the speed error (ω_{err}), the DFIG has an additional block called 'pitch compensation' which provides pitch angle error signal in response to the deviation of output power from the rated value. When the power output increases beyond the rated value, the

pitch compensator acts to increase the pitch angle and brings the power back to the rated value.

The torque command (T_{set}) is used to compute active power order (P_{ord}) which in turn provides excitation current to the rotor side converter. In other words, the turbine control model sends a power order signal to the electrical control, requesting that the converter deliver this power to the grid. The maximum active power order (P_{max}) from the controller is limited by the active power limiter block shown in Figure 3.3. The current command (I_p) is computed by dividing P_{ord} from the wind turbine model by the generator terminal voltage (V_t). The current command is limited by the short term current capability of the converter ($I_{p\text{-}max}$).

The overall DFIG model comprising the details of the default control blocks together with the parameter values that have been used for the present work is shown in Figure 3.4. This work uses TSAT and SSAT, the two commercial software packages within which the model is available. These tools are used to test the large test system utilized in the present work.

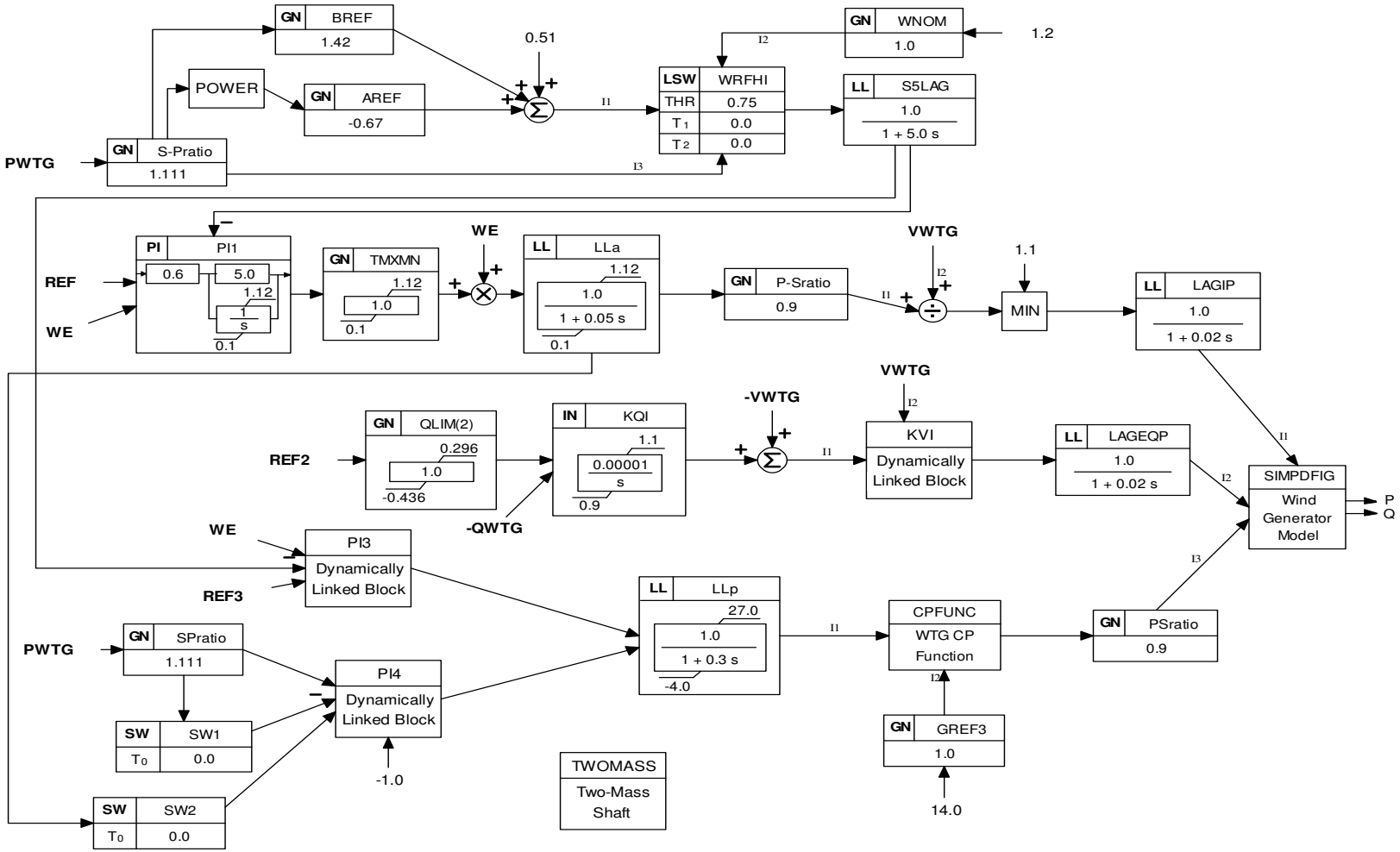

Figure 3.4 DFIG model implemented in TSAT [48]

CHAPTER 4

IMPACTS OF WIND POWER PENETRATION ON POWER SYSTEM STABILITY

Power system stability is the property of a power system that ensures the stable operating equilibrium under normal conditions and restores an acceptable state of equilibrium when the system is subjected to a disturbance [50]. The ability of the network to cope with these disturbances and to restore the normal operating condition is addressed by stability studies. In order to obtain satisfactory system operation, synchronous machines that represents major portion of the electrical power generation should remain in synchronism. One of the major factors governing the stability is the dynamics of generator rotor angles and power-angle relationships [50].

In an interconnected system, the ability to restore equilibrium between electromagnetic torque and mechanical torque is determined by the rotor angle stability of each synchronous machine. With the increased number of wind farms in operation, which are asynchronous in nature, the system experiences change in dynamic characteristics. Moreover, for wind power generation, the kinetic energy in wind is translated into mechanical torque. The characteristics associated with exploitation of wind energy and components used for power conversion does contribute to change in system dynamics.

Following a perturbation, the change in electromagnetic torque of the synchronous machine can be explained by two torque components, namely, the syn-

chronizing torque component and the damping torque component. System stability depends on the existence of both components of torque for each of the synchronous machines [49]. Insufficient synchronizing torque results in non-oscillatory instability whereas insufficient damping torque results in oscillatory instability. In order to simplify the analysis of stability problems, the rotor angle stability is further categorized into transient stability and small signal stability. These categories of instability in response to the penetration of wind power are discussed in the following sections.

4.1 Transient stability

Transient stability is the ability of a power system to maintain synchronism when subjected to a severe disturbance. Severe network disturbances include equipment outages, load changes or faults that result in large excursion of generator rotor angles. The resulting system response is influenced by the nonlinear power angle relationship. Transient stability depends on both the initial operating state of the system and the severity of the disturbance. Instability is usually caused due to insufficient synchronizing torque and results in aperiodic angular separation. The time frame of interest in transient stability studies is usually 3 to 5 seconds following the disturbance. The duration may extend up to 10-20 seconds for a very large system with dominant inter-area swings [49].

In a synchronous machine, if during a network disturbance the electrical torque falls below the mechanical torque, the rotor will accelerate causing the increase in rotor speed and angular position of the rotor flux vector. Since the in-

crease in rotor angle results in an increase in the generator load torque, a mechanism exists to increase the electrical torque so as to match the mechanical torque. In the case of DFIGs, generator load disturbances also give rise to variations in the speed and the position of the rotor. However, due to the asynchronous operation involved, the position of the rotor flux vector is not dependent on the physical position of the rotor and the synchronizing torque angle characteristic does not exist [16]. The transient stability of a system with wind turbines also depends on factors such as fault conditions and network parameters. Wind speed, however, is assumed to be constant in transient stability simulations involving wind turbines. The mechanical power, on the other hand, is not constant as it depends on wind speed as well as the generator speed [21].

4.2 Small signal stability

Small signal stability is defined as the ability of the power system to maintain synchronism when subjected to small disturbances [50]. The disturbance is regarded as small if the equations describing the system response can be linearized for the purpose of analysis. The small signal stability problem normally occurs due to insufficient damping torque which results in rotor oscillations of increasing amplitude [50]. The following general equations can be used to describe the dynamics of the power system,

$$\dot{\boldsymbol{x}} = \boldsymbol{h}(\boldsymbol{x},\boldsymbol{u},t) \tag{4.1}$$

$$\boldsymbol{y} = \boldsymbol{g}(\boldsymbol{x},\boldsymbol{u}). \tag{4.2}$$

For small signal stability analysis, the nonlinear equations of the dynamic power system are first linearized around a specific operating point. The resulting set of linear differential equations describes the dynamic behavior of the power system subject to a small disturbance around this operating point. The linearized equation is of the form,

$$\Delta \dot{x}_i = \frac{\partial h_i}{\partial x_1}\Delta x_1 + \cdots + \frac{\partial h_i}{\partial x_n}\Delta x_n + \frac{\partial h_i}{\partial u_1}\Delta u_1 + \cdots + \frac{\partial h_i}{\partial u_r}\Delta u_r \tag{4.3}$$

$$\Delta y_j = \frac{\partial g_j}{\partial x_1}\Delta x_1 + \cdots + \frac{\partial g_j}{\partial x_n}\Delta x_n + \frac{\partial g_j}{\partial u_1}\Delta u_1 + \cdots + \frac{\partial g_j}{\partial u_r}\Delta u_r \tag{4.4}$$

where, n is the order of the system and r is the number of inputs. The linearized equation can be written in the form,

$$\boldsymbol{\Delta \dot{x}} = \boldsymbol{A\Delta x} + \boldsymbol{B\Delta u} \tag{4.5}$$

$$\boldsymbol{\Delta y} = \boldsymbol{C\Delta x} + \boldsymbol{D\Delta u} \tag{4.6}$$

where, ***A, B, C*** and ***D*** are known as state or plant matrix, input matrix, output matrix and feed forward matrix respectively.

The state equation in the frequency domain can be obtained by performing the Laplace transform of the above equation as follows,

$$s\boldsymbol{\Delta x}(s) - \boldsymbol{\Delta x}(0) = \boldsymbol{A\Delta x}(s) + \boldsymbol{B\Delta u}(s) \tag{4.7}$$

$$\boldsymbol{\Delta y}(s) = \boldsymbol{C\Delta x}(s) + \boldsymbol{D\Delta u}(s) \tag{4.8}$$

$$(s\boldsymbol{I} - \boldsymbol{A})\boldsymbol{\Delta x}(s) = \boldsymbol{\Delta x}(0) + \boldsymbol{B\Delta u}(s). \tag{4.9}$$

Equation 4.9 is defined as the characteristic equation of matrix *A*. The values of *s* which satisfy the characteristic equation are known as the eigenvalues of matrix ***A***. Matrix ***A*** consists of the partial derivatives of the function ***h*** with respect to the state variables. The eigenvalues of matrix ***A***, thus exhibit important

information about the system response to small perturbations and thus characterize the stability of the system [50]. The change in design and operating condition of the power system is reflected in the eigenvalues of the system state matrix.

The time dependent characteristic of a mode corresponding to an eigenvalue λ is given by $e^{\lambda t}$. A real positive eigenvalue determines an exponentially increasing behavior while a negative real eigenvalue represents a decaying mode. A complex eigenvalue with positive real part results in an increasing oscillatory behavior and one with a negative real part results in damped oscillation. The real component of the eigenvalue gives the damping and the imaginary component gives the frequency of oscillation. The frequency of oscillation (f) and damping ratio (ξ) of a complex eigenvalue ($\lambda=\sigma+j\omega$) can be represented as,

$$f = \frac{\omega}{2\pi} \tag{4.10}$$

$$\xi = \frac{-\sigma}{\sqrt{\omega^2 + \sigma^2}}. \tag{4.11}$$

The damping ratio determines the rate of decay of the amplitude of the oscillation. An eigenvalue of the state matrix $\boldsymbol{A}$ and the associated right eigenvector ($\boldsymbol{v_i}$) and left eigenvector ($\boldsymbol{w_i}$) are defined as,

$$\boldsymbol{A}\boldsymbol{v}_i = \boldsymbol{v}_i\lambda_i \tag{4.12}$$

$$\boldsymbol{w}_i\boldsymbol{A} = \lambda_i\boldsymbol{w}_i. \tag{4.13}$$

The component of the right eigenvector gives the mode shape, that is, the relative activity of the state variables when a particular mode is excited. For example, the degree of activity of the state variable x_j in the i^{th} mode is given by v_{ji} of right eigenvector $\boldsymbol{v_i}$. *The* j^{th} element of the left eigenvector $\boldsymbol{w_i}$ weighs the con-

tribution of this activity to the i^{th} mode. The participation factor of the j^{th} state variable (x_j) in the i^{th} mode is defined as the product of the j^{th} component of the right and left eigenvectors corresponding to the i^{th} mode,

$$p_{ji} = v_{ji} w_{ij}. \tag{4.14}$$

In large power systems, the small-signal stability problem can be either local or global in nature. Power system oscillations are usually in the range between 0.1 and 2 Hz depending on the number of generators involved. Local oscillations lie in the upper part of the range and consist of the oscillation of a single generator or a group of generators against the rest of the system [26]. Stability (damping) of these oscillations depends on the strength of the transmission system as seen by the power plant, generator excitation control systems and plant output [50]. In contrast inter area oscillations are in the lower part of the frequency range representing oscillations among the group of generators. Load characteristics, in particular, have a major effect on the stability of inter area modes [50]. The time frame of interest in small signal stability studies is of the order of 10-20 seconds following a disturbance [49].

The DFIG based design consisting of the power electronics converter imparts significant effect on the dynamic performance of the system. The important point to note is that the DFIGs are asynchronous machines but the machines inject power into the system and as a result will affect the angular positions of all the other synchronous generators. In addition DFIGs do not contribute to the inertia in the system. Hence, the synchronizing capability of the synchronous generators

in the system will be affected. This leads to a significant impact on the electro-mechanical modes of oscillation. Thus, the following section discusses on how the change in system parameter can affect the electromechanical modes of oscillations of the system.

4.2.1. Eigenvalue sensitivity

The effect of the system parameters on the overall system dynamics can be examined by evaluating the sensitivity of the eigenvalues with respect to variations in system parameters [51,52,53,54]. This section presents the mathematical derivation of the sensitivity of eigenvalue with respect to the system parameter x_j.

Taking partial derivative of (4.12) with respect to x_j on both sides,

$$\frac{\partial \boldsymbol{A}}{\partial x_j}\boldsymbol{v}_i + \boldsymbol{A}\frac{\partial \boldsymbol{v}_i}{\partial x_j} = \lambda_i \frac{\partial \boldsymbol{v}_i}{\partial x_j} + \frac{\partial \lambda_i}{\partial x_j}\boldsymbol{v}_i \tag{4.15}$$

where, $\boldsymbol{A}$ is an $n \times n$ state matrix, λ_i is the i^{th} eigenvalue, $\boldsymbol{v_i}$ is an $n \times 1$ right eigenvector of $\boldsymbol{A}$ corresponding to λ_i and n is the order of the system.

Pre-multiplying (4.15) by w_i yields,

$$\boldsymbol{w}_i \frac{\partial \boldsymbol{A}}{\partial x_j}\boldsymbol{v}_i + \boldsymbol{w}_i A\frac{\partial \boldsymbol{v}_i}{\partial x_j} = \boldsymbol{w}_i \lambda_i \frac{\partial \boldsymbol{v}_i}{\partial x_j} + \boldsymbol{w}_i \frac{\partial \lambda_i}{\partial x_j}\boldsymbol{v}_i \tag{4.16}$$

where, $\boldsymbol{w_i}$ is the $1 \times n$ left eigenvector of $\boldsymbol{A}$ corresponding to λ_i.

Rearranging (4.15),

$$\boldsymbol{w}_i \frac{\partial \boldsymbol{A}}{\partial x_j}\boldsymbol{v}_i + \boldsymbol{w}_i\left(\boldsymbol{A} - \lambda_i \boldsymbol{I}\right)\frac{\partial \boldsymbol{v}_i}{\partial x_j} = \boldsymbol{w}_i \frac{\partial \lambda_i}{\partial x_j}\boldsymbol{v}_i. \tag{4.17}$$

Again,

$$\boldsymbol{w}_i\left(\boldsymbol{A} - \lambda_i \boldsymbol{I}\right) = 0. \tag{4.18}$$

Substituting (4.18) in (4.17) yields,

$$\boldsymbol{w}_i \frac{\partial \boldsymbol{A}}{\partial x_j} \boldsymbol{v}_i = \boldsymbol{w}_i \frac{\partial \lambda_i}{\partial x_j} \boldsymbol{v}_i . \tag{4.19}$$

Rearranging (4.19) yields,

$$\frac{\partial \lambda_i}{\partial x_j} = \frac{\boldsymbol{w}_i \dfrac{\partial \boldsymbol{A}}{\partial x_j} \boldsymbol{v}_i}{\boldsymbol{w}_i \boldsymbol{v}_i} . \tag{4.20}$$

Thus, sensitivity of the eigenvalue λ_i to the system parameter x_j is given by (4.20). This expression will be used further to explore the impact of inertia of the DFIGs replaced by round rotor synchronous machines of equivalent rating on the damping ratio of various modes of oscillation.

4.3 Frequency control and inertia

In any power system, frequency is controlled by balancing the power generation against load demand on a second-by-second basis. There is a need for continuous adjustment of generator output as the load demand varies. At the same time, the system should be able to respond to occasional larger mismatches in generation and load caused, for example, by the tripping of a large generator or a large load.

Whenever there is load/generation imbalance, synchronous generators in a system respond in three stages to bring the system back to normal operation. The initial stage is characterized by the release or absorption of kinetic energy of the rotating mass – this is a physical and inherent characteristic of synchronous generators. For example, if there is sudden increase in load, electrical torque increases to supply load increase, while mechanical torque of the turbine initially remains

constant. Hence, the acceleration, α, given by $J\alpha = T_m - T_e$ becomes negative. The turbine-generator decelerates and rotor speed drops as kinetic energy is released to supply the load change. This response is called “inertial response”. As the frequency deviation exceeds certain limit, the turbine-governor control will be activated to change the power input to the prime mover. The rotor acceleration eventually becomes zero and the frequency reaches a new steady state. This is referred to as “primary frequency control”. After primary frequency support, there still exists steady state frequency error. To remove the error, the governor set points are changed and the frequency is brought back to nominal value. This is called “secondary frequency control”. These three phenomena take place in succession in any system to restore the normal operating equilibrium.

The inertia of wind turbines is comparable to that of conventional synchronous generators. In fixed speed wind turbine systems with uncontrolled squirrel cage rotors, this inertia of the turbine is automatically available as the frequency of the grid tends to decrease following a fault or loss of generation or transmission line. Under such condition, the speed of the turbine reduces and part of stored energy is fed into the system through the induction generator.

However, in the case of DFIG units, their dynamic performance as seen by the grid is completely governed by the power electronic converters that control them. With conventional control, where rotor currents are always controlled to extract maximum energy from the wind by varying the rotor speed, the inertia of the turbine is effectively decoupled from the system. With the penetration of

DFIG based wind farms, the effective inertia of the system will be reduced. With the inertia decreasing due to a large number of DFIG wind turbines in operation, system reliability following large disturbances could be significantly affected.

CHAPTER 5

PROPOSED APPROACH

This dissertation encompasses the study and mitigation of increased penetration of wind turbine generators on the small signal and transient stability of the system. The study is conducted using DSA^{Tools}, a suite of analytical tools developed by Powertech Labs Inc., namely, power flow and short circuit analysis tool (PSAT), transient security assessment tool (TSAT) and small signal analysis tool (SSAT).

The power flow solution from PSAT provides the initial operating condition for the power system. The solution obtained from power flow provides initial conditions for the dynamic simulation. The dynamic simulation for the present work encompasses transient stability study and small signal stability study.

5.1 Small signal stability assessment

The basis of this study lies on the premise that with the penetration of DFIG based wind farms the effective inertia of the system will be reduced. In this regard, a first step proposed towards studying the system behavior with increased DFIG penetration is to identify how the small signal stability behavior changes with the change in inertia. The approach is thus intended to evaluate eigenvalue sensitivity with respect to generator inertia. From (4.20), the eigenvalue sensitivity with respect to inertia can be expressed as,

$$\frac{\partial \lambda_i}{\partial H_j} = \frac{\boldsymbol{w}_i \frac{\partial \boldsymbol{A}}{\partial H_j} \boldsymbol{v}_i}{\boldsymbol{w}_i \boldsymbol{v}_j} \tag{5.1}$$

where, H_j is the inertia of j^{th} conventional synchronous generator, λ_i is the i^{th} eigenvalue $\boldsymbol{w_i}$ and $\boldsymbol{v_i}$ is the left and right eigenvector corresponding to i^{th} eigenvalue respectively.

The eigenvalue sensitivity had been addressed as early as the 1960s [51]. However, the key to the proposed analysis is to examine the sensitivity with respect to inertia and identify which modes are affected in a detrimental fashion and which modes are benefitted by the increased DFIG penetration.

The important point to note is that with the increased penetration of DFIG, the synchronizing capability of the synchronous generators in the system will be affected. This leads to a significant impact on the electromechanical modes of oscillation. The proposed method provides a means of quantifying the effect of reduced inertia on the damping ratio of various modes of oscillation. This is a novel approach and has not been addressed in the literature so far. The following steps are adopted while evaluating the system response with respect to small disturbances:

- Replace all the DFIGs with conventional synchronous generators of the same MVA rating which will represent the base case operating scenario for the assessment.
- Perform eigenvalue analysis in the frequency range: 0.1 to 2 Hz and damping ratio below 2.5%.

- Evaluate the sensitivity of the eigenvalues with respect to inertia (H_j) of each wind farm represented as a conventional synchronous machine which is aimed at observing the effect of generator inertia on dynamic performance.
- Perform eigenvalue analysis for the case after introducing the existing as well as planned DFIG wind farms in the system.

5.2 Transient stability assessment

The machine rotor angle measured with respect to a synchronously rotating reference is considered as one of the parameters to test stability of the system. If the difference in relative angle between the machines increases indefinitely, the system is unstable. The severity of a contingency and the trajectory of a system following a disturbance can be assessed by evaluating the transient stability index (*TSI*). The *TSI* is obtained from the transient security assessment tool (TSAT) which calculates the index based on angle margin algorithm as follows [48],

$$TSI = \frac{360 - \delta_{\max}}{360 + \delta_{\max}} \times 100 \qquad -100 < TSI < 100 \qquad (5.2)$$

where, δ_{max} is the maximum angle separation of any two generators in the system at the same time in the post-fault response. $TSI > 0$ and $TSI \leq 0$ correspond to stable and unstable conditions respectively.

The objective of transient stability analysis here is to examine if the modes identified in the small signal stability analysis can be excited by the large distur-

bance and analyze the transient stability performance. Each critical mode obtained in the small signal stability study is scrutinized in time domain.

5.3 Frequency support from a DFIG

5.3.1. Modification of torque set point

The proposed strategy is based on the idea of changing the torque set point of the DFIG for changes in grid frequency. The schematic of the supplementary control proposed in the present work in shown in Figure 5.1. From Figure 3.3 and Figure 5.1, it is revealed that the supplementary control signal (ΔT_{set}) is algebraically added to the torque set point (T_{set}). The torque set point increases whenever grid frequency drops from the nominal value of 1 p.u.

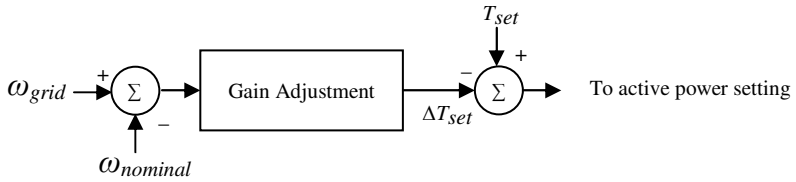

Figure 5.1 Supplementary control loop

The input to the supplementary controller is the frequency deviation at the point of interconnection. The study is carried out in a system which consists of several wind farms dispersed geographically. During the first few seconds, even the same disturbance can have wide ranges of impact on the machines involved. Hence, transiently, the frequency deviation might vary at different buses in the system. As the controller is required to respond accordingly, the deviation of grid frequency is used as a control input. In addition, the support from the DFIGs is dependent on the kinetic energy stored in the turbine blades. This support is li-

mited by the inertia constant of the turbines which in turn depends on its MVA rating. Hence, the gain of the supplementary control block is adjusted based on the frequency deviation and MVA rating of the wind farm. The gain is evaluated as follows,

$$G = \frac{1}{\Delta\omega_{\max}} \frac{S_{BM}}{S_{B,sys}} \tag{5.3}$$

where, G is the gain of the supplementary control loop, S_{BM} is the rated MVA of the DFIG wind farm, $S_{B,sys}$ is the system MVA base, and $\Delta\omega_{max}$ is the maximum deviation in grid frequency at the point of interconnection among all the wind farms. The maximum deviation in grid frequency is evaluated by simulating a series of large disturbances in terms of generation drops that the system can withstand without being transiently unstable.

When the objective is to provide inertial support, the time frame of interest is the first few seconds after the disturbance. The DFIG equipped with the supplementary control loop can support the system during this period. The additional electrical power output is provided via a concomitant reduction in rotor speed. Furthermore, as the primary input, the wind flow, cannot be changed, kinetic energy stored in the rotating mass of a wind turbine is assumed to provide primary frequency control. This, however, depends on several factors such as rating and margin on the converter and the aerodynamics of the turbine. Due to the limited stored kinetic energy, the support can only be provided for a short period of time. The final steady state frequency error, if it is non zero, should be adjusted by sec-

ondary frequency control as discussed in Section 4.3. As the supplementary control is not aimed at correcting the steady state error, proportional gain suffices.

5.3.2. Adjustment of pitch compensation

Owing to variable speed operation, the stored kinetic energy and, accordingly, the inertial response of the DFIG is dependent on the captured mechanical power. The latter is governed by the pitch angle controller. The maximum benefit can be achieved when the pitch angle controller aids the operation of the supplementary frequency controller. Conventional parameters of pitch angle controller can be tailored so that mechanical power can be changed thus providing primary frequency response under transient condition. This is done by suitably varying the PI controller gain of the pitch compensator. The parameters should be varied in such a way that the pitch compensator does not act to increase the pitch angle during the transient period when the system is subjected to loss of generation.

A heuristic approach based on trial and error [55] is used. The “cause and effect” approach is adopted when the controller is tuned. The parameters are selected such that pitch compensator reduces the pitch angle thus avoiding the transient drop in extracted mechanical power during the condition when system demands more active power. This action aids the purpose of supplementary controller thus increasing the power output during the transient with response to drop in grid frequency.

5.3.3. Adjustment of maximum power order

The additional power supplied by the DFIG depends on P_{max} which in turn depends on factors such as the rating and margin on the converter and the aerodynamics of the turbine. The idea here is to increase the value of P_{max} such that inertial response of DFIG is improved during the transient event. To be within the converter design limits, the increased value of P_{max} should not demand the current command beyond the short term current capability of the converter (I_{pmax}). The value of P_{max} selected in this dissertation allows for 20% increase in power output beyond rated which is also consistent with the work carried out in [40].

5.4 DFIG PSS and oscillation damping

The PSS employed for DFIGs in this work consists of wind generator power output as its input. The active power command is modulated in phase opposition to the power system oscillation and is fed to the active power control loop of the DFIG as shown in Figure 3.3. The schematic of the proposed control is shown in Figure 5.2. An additional control block with the DFIG terminal voltage as PSS input signal is fed to the reactive power control loop. The respective signals are then fed through the washout block which acts as a high pass filter to eliminate any control contribution under steady condition. The signal is then fed through compensator that provides appropriate gain and contributes to system damping.

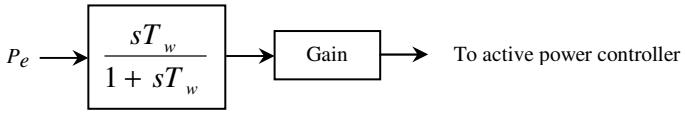

Figure 5.2 Schematic of DFIG PSS

The electrical behavior of the generator and converter is that of a current regulated voltage source converter. The conventional aspects of generator performance related to internal angle, excitation voltage and synchronism are largely irrelevant. Consequently, there is no considerable lag in the signal through the converter. This rules out the need for the phase compensation block while adjusting the DFIG excitation to improve the damping.

5.5 System description

The study is carried out on a large system having over 22000 buses, 3104 generators with a total generation of 580,611 MW. All the modeling details provided within the base set of data are retained and represented in the analysis. This includes the modeling of governors on conventional generators. Within this large system, the study area which is experiencing a large increase of wind penetration has a total installed capacity of 4730.91 MW. The analysis is based on the information provided with regard to the existing and planned increases in wind penetration. A total of 14 wind farms ranging from 14 MW to 200 MW with a total installed capacity of 1460 MW are modeled as DFIGs. This information is used to set up the changed cases from the base case provided.

The system has transmission voltage levels ranging from 34.5 kV, 69 kV, 161 kV to 345 kV. WTGs are connected to the grid at the 69 kV level. All new

wind farms are represented using the GE 1.5 MW DFIG model available in TSAT. Each DFIG unit has a rated power of 1.5 MW and MVA rating of 1.67 MVA. The reactive power capability of each unit corresponds to the power factor in the range +0.95/-0.90 which corresponds to Q_{max} = 0.49 MVAr and Q_{min} = -0.73 MVAr.

CHAPTER 6

RESULTS AND DISCUSSION

This chapter presents the results of simulations carried out for two different study objectives, namely, small signal stability and transient stability. Different forms of disturbances excite the system in different ways and have wide ranges of impact on the machines involved. With the objective of observing the system response for small and large disturbances, the same base case operating scenario is considered for small signal stability and transient stability study cases. Hence, the area and machines considered for small signal stability study is also considered for transient stability study.

6.1 Scenario description

Four different cases are analyzed. The description of each case is provided below:

- Case A constitutes the case wherein all the existing DFIGs in the study area in the original base case are replaced by conventional round rotor synchronous machines (GENROU) of equivalent MVA rating.
- The original base case provided with existing DFIGs in the system is referred to as Case B.
- Case C constitutes the case wherein the penetration of DFIG based WTGs in the study area is increased by 915 MW. The load in the study area is increased by 2% (predicted load growth) and rest of the generation increase is exported to a designated nearby area.

- Case D constitutes the case wherein the DFIG wind farms with the increased wind penetration are replaced by GENROU of corresponding MVA rating. Thus, in Case D the GENROU machines representing the WTGs are of higher MVA rating than in Case A.

The export of increased power from the study area is aimed at keeping the total system power generation constant. This implies that the power export from the study area to the neighboring area is implemented by the concomitant reduction in the generated power in the neighboring area by the same amount.

6.2 Small signal stability

The basis of this study lies in the premise that with the penetration of DFIG based wind farms the effective inertia of the system will be reduced. Hence, as a first step towards studying the system behavior with increased DFIG penetration and to evaluate how the eigenvalues respond to the change in inertia, a sensitivity analysis should be carried out with respect to generator inertia.

6.2.1. Sensitivity analysis with respect to inertia

The eigenvalue sensitivity with respect to a specific system parameter indicates the degree to which a change in particular parameter affects the eigenvalues. The sensitivity analysis with respect to inertia is only conducted for Case A where all machines in the system are represented by conventional synchronous generators. The sensitivity of a given mode with respect to inertia of each wind farm replaced by a conventional synchronous generator is obtained. The sensitivi-

ty is evaluated by computing a pair of modes, one of them with the value of inertia in the base case and the other with a "perturbed" value. When computing the mode in the perturbed case, the inertia is increased by 0.5%. The computation is performed using an available feature in SSAT. This feature allows for the evaluation of sensitivity with respect to a wide range of parameters. In this analysis inertia was chosen to be the sensitivity parameter. The analysis inherently accounts for the insertion points of the wind farms in the system.

The analysis is carried out only for Case A, for all modes in a range of frequencies from 0.1 Hz to 2 Hz. As the stability of a mode is determined by the real part of eigenvalue, the sensitivity of the real part is examined and the mode which has the largest real part sensitivity to change in inertia is identified. Among the several modes of oscillation analyzed, the result of sensitivity analysis associated with the mode having significant detrimental real part sensitivity, in comparison to the real part of the eigenvalue is shown in Table 6.1.

Table 6.1 Dominant mode with detrimental effect on damping

Real (1/s)	Imaginary (rad/s)	Frequency (Hz)	Damping ratio (%)
-0.0643	3.5177	0.5599	1.83

The corresponding sensitivity values for the real part of this mode with respect to each of the 14 wind farm generators replaced by conventional synchronous machines of the same MVA rating are shown in Table 6.2. The real part sensitivities all having negative values as shown in Table 6.2 reveal that with the decrease in inertia at these locations, the eigenvalue will move towards the positive

right half plane making the system less stable. Participation factor analysis for this mode shows that altogether 26 machines participate in the mode. Participation factors corresponding to each machine are shown in Figure 6.1.

Table 6.2 Eigenvalue sensitivity corresponding to the dominant mode with detrimental effect on damping

No.	Generator bus #	Base value of inertia (s)	Sensitivity of real part ($1/s^2$)
1	32672	2.627	-0.0777
2	32644	5.7334	-0.0355
3	32702	3	-0.0679
4	32723	5.548	-0.0367
5	49045	5.2	-0.0383
6	49050	4.6	-0.0444
7	49075	4.2	-0.0475
8	52001	5.2039	-0.0389
9	55612	3.46	-0.0581
10	55678	4.3	-0.0467
11	55881	4	-0.0506
12	55891	4.418	-0.0466
13	55890	5.43	-0.037
14	55889	5.43	-0.0374

The next step in the analysis is to observe if the penetration of DFIGs has beneficial impact in terms of damping power system oscillations. The sensitivity with respect to inertia is examined for positive real part sensitivity. This identifies the mode where the increased penetration of DFIGs in the system results in shifting the eigenvalues of the system state matrix towards the negative half plane. Among the several modes of oscillation analyzed, the result of sensitivity analysis

associated with the mode having the largest positive real part sensitivity is shown in Table 6.3.

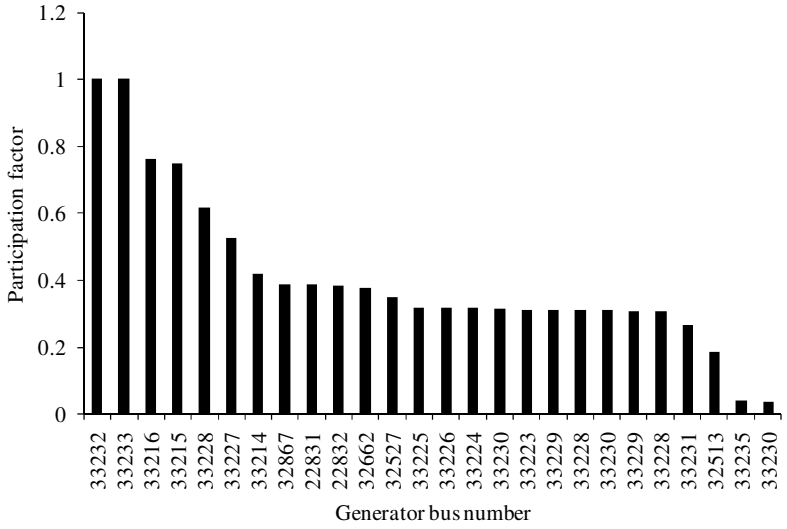

Figure 6.1 Participation factor corresponding to the generator speed state for the dominant mode with detrimental effect on damping

Table 6.3 Dominant mode with beneficial effect on damping

Real (1/s)	Imaginary (rad/s)	Frequency (Hz)	Damping ratio (%)
-0.0651	2.8291	0.4503	2.3

The corresponding real part sensitivity values for each of the 14 wind farm generators represented by conventional synchronous machines are shown in Table 6.4. The real part sensitivities are all positive in sign indicating that with the decrease in inertia at each of these locations the mode will move further into the left half plane making the system more stable. The participation factor analysis shows that 34 machines participate in this mode. The participation factors corresponding to each machine are shown in Figure 6.2.

Table 6.4 Eigenvalue sensitivity corresponding to the dominant mode with beneficial effect on damping

No.	Generator bus #	Base value of inertia (s)	Sensitivity of real part ($1/s^2$)
1	32672	2.627	0.0169
2	32644	5.7334	0.0078
3	32702	3	0.015
4	32723	5.548	0.008
5	49045	5.2	0.0075
6	49050	4.6	0.0092
7	49075	4.2	0.0104
8	52001	5.2039	0.0079
9	55612	3.46	0.0125
10	55678	4.3	0.0098
11	55881	4	0.0107
12	55891	4.418	0.0095
13	55890	5.43	0.0082
14	55889	5.43	0.008

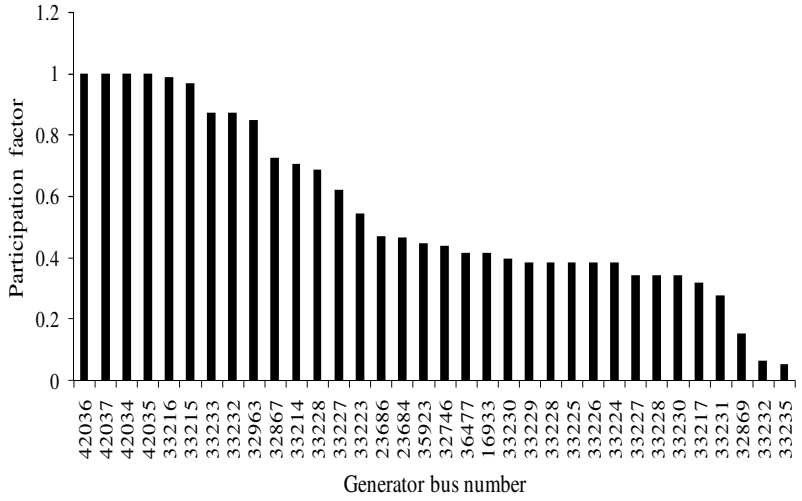

Figure 6.2 Participation factor corresponding to the generator speed state for the dominant mode with beneficial effect on damping

6.2.2. Eigenvalue analysis with DFIG penetration

Detailed eigenvalue analysis is conducted for Cases A to D in the frequency range of 0.1 Hz to 2 Hz to substantiate the results of the sensitivity analysis. Table 6.5 shows the result of eigenvalue analysis corresponding to the mode listed in Table 6.1 which has detrimental impact with increased DFIG penetration.

The critical mode is observed in all the four cases. The frequency of the mode is relatively unchanged. It is observed that the damping ratio associated with the mode is reduced from 1.83% in Case A to 1.16% in Case B. The damping ratio has further reduced to 0.68% in the Case C. However, in Case D with DFIGs replaced by conventional machines the damping ratio is improved to 1.22%.

Table 6.5 Result summary for cases A, B, C and D for dominant mode with detrimental effect on damping

Case	Real (1/s)	Imaginary (rad/s)	Frequency (Hz)	Damping ratio (%)	Dominant machine
A	-0.0643	3.5177	0.5599	1.83	33232
B	-0.0412	3.5516	0.5653	1.16	33232
C	-0.0239	3.5238	0.5608	0.68	33232
D	-0.0427	3.4948	0.5562	1.22	33232

The change in damping ratio due the increased penetration of DFIGs accurately reflects the trend indicated by sensitivity analysis. In Cases B and C where the inertia is reduced due to the inclusions of DFIGs the damping has dropped. In Cases A and D where the machines are represented as conventional synchronous machines of equivalent rating the damping is higher. The increased flow into the

neighboring area does not affect this mode whereas the change in inertia significantly affects the damping of this mode.

A total number of 26 dominant machines participate in the mode of oscillation in Case A. In Case B, the number of machines participating in the mode increases to 32. In Case C the number of machines participating in the mode further increased to 33. However, the number of machines participating in the mode of oscillation for Case D is 27. This analysis indicates a trend that with the increased penetration of DFIGs in the system, more machines are affected and they participate in the mode of oscillation.

In the course of the modal analysis in the frequency range considered, another mode, which is not observed in Case A and Case B is observed only in Cases C and D and is found to have low damping. The results corresponding to this mode are shown in Table 6.6. It appears that this mode manifests itself largely as a result of the increased exports to the neighboring area. The machines participating in the mode shown in Table 6.6 with their corresponding participation factor are shown in Figure 6.3.

Table 6.6 Result summary between cases C and D for dominant mode with detrimental effect on damping with increased exports

Case	Real (1/s)	Imaginary (rad/s)	Frequency (Hz)	Damping ratio (%)	Dominant machine
C	-0.0663	3.9097	0.6223	1.7	32963
D	-0.0304	3.7911	0.6034	0.8	32963

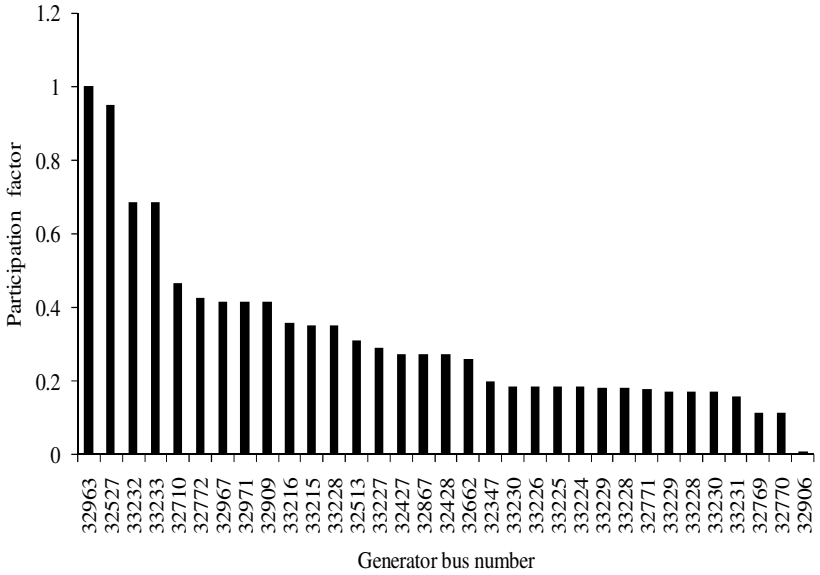

Figure 6.3 Participation factor corresponding to the generator speed state for the dominant mode shown in Table 6.6

The eigenvalue analysis carried out for the mode with beneficial eigenvalue sensitivity is shown in Table 6.7. The damping ratio associated with the mode having a beneficial impact has increased from 2.3% in the Case A to 2.55% in the Case B. It is also observed that the damping ratio has further improved to 2.68% in the Case C. However, in Case D with DFIGs replaced by conventional machines the damping ratio is reduced to 2.02%. These results again reflect the trend in damping change identified by the sensitivity analysis and also show the small change in damping as reflected by the sensitivity values in comparison to the mode which was detrimentally affected by the change in inertia.

These results reveal that the eigenvalue sensitivity with respect to inertia provides an effective measure of evaluating the impact of DFIG penetration on the system dynamic performance. The detailed eigenvalue analysis carried out for each of the four cases is found to substantiate the results obtained from sensitivity

analysis. The proposed method is found to be valid for identifying both the beneficial as well as the detrimental impact due to increased DFIG penetration.

Table 6.7 Result summary for cases A, B, C and D for the dominant mode with beneficial effect on damping

Case	Real (1/s)	Imaginary (rad/s)	Frequency (Hz)	Damping ratio (%)	Dominant machine
A	-0.0651	2.8291	0.4503	2.3	42037
B	-0.0725	2.8399	0.452	2.55	33216
C	-0.0756	2.8189	0.4486	2.68	42037
D	-0.0566	2.805	0.4464	2.02	42037

6.3 Transient stability analysis

In conducting the transient stability analysis, the objective is to examine if the modes with low damping observed in the small signal analysis could be excited by a large disturbance. In order to identify the disturbance location which will excite the specific mode, the network structure around the machines with the largest participation factors in the specific mode is examined. Simulations are conducted for various three phase faults at several buses followed by outage of the line connected to the faulted bus. The fault is cleared at a suitable time depending on the bus voltage level.

6.3.1. Fault scenario 1 - Detrimental impact on system performance

The bus structure near the generator 33232 which has the largest participation factor (see Figure 6.1) in the mode detrimentally affected by the penetration of DFIGs (see Table 6.1) is shown in Figure 6.4.

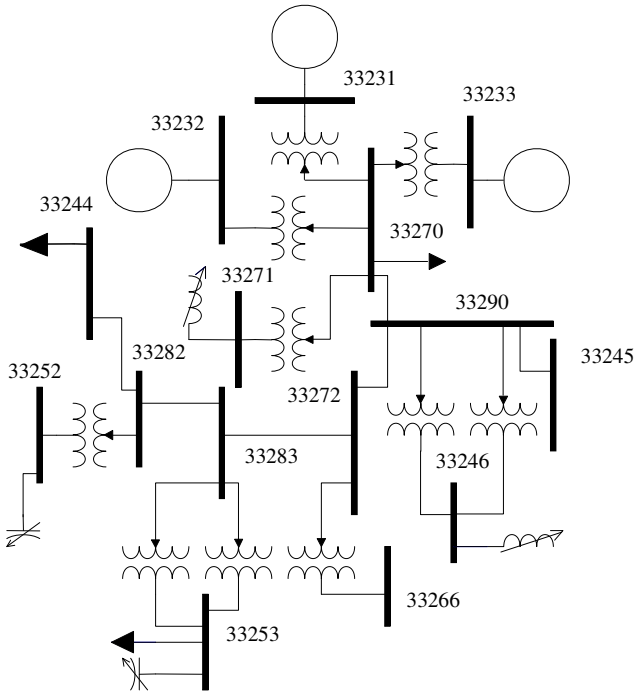

Figure 6.4 Single line diagram showing the bus structure near a generator with highest participation factor

The objective here is to observe if a large disturbance near generator 33232 will excite the mode shown in Table 6.1. A three phase fault is applied at bus 33283 which is a 230 kV bus and is cleared after 5 cycles. The fault is cleared followed by the clearing of the line connecting the buses 33283 and 33282.

As the dominant mode considered from small signal analysis corresponds to the speed state of the machines, the generator speed is observed in time domain. Figure 6.5 shows the generator speed corresponding to the generator 32527 which is one of the machines participating in the mode as shown in Figure 6.1. Observing the oscillation corresponding to the last swing of Figure 6.5, the least amount of damping is found in Case C which is followed by Case B and Case D. The damping is found to be the highest in Case A. The damping behavior ob-

served in time domain corresponds exactly to the damping ratio provided by the eigenvalue analysis in Table 6.5. This fault scenario is thus found to have detrimental impact on system performance with respect to increased wind penetration.

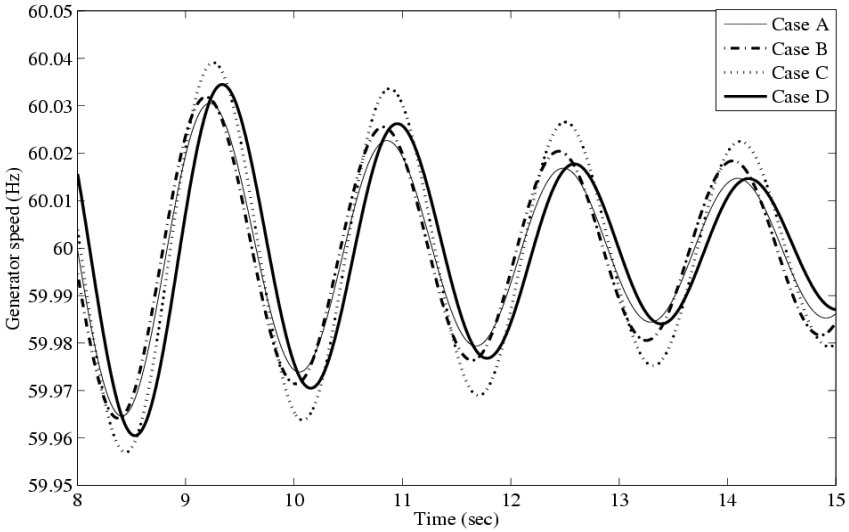

Figure 6.5 Bus 32527 generator speed for Cases A, B, C and D

6.3.2. Fault scenario 2 - Examine low damping mode with increased export

The bus structure near the generator at bus 32963 is shown in Figure 6.6. This is the generator which has the largest participation factor (see Figure 6.3) in the mode given in Table 6.6. The objective here is to observe if a large disturbance near generator 32963 will excite the mode shown in Table 6.6 and reflect the result obtained from small signal stability. A three phase fault is applied at bus 32946 which is at 345 kV. The fault is cleared after 4.5 cycles followed by clearing the line connecting the buses 32969 and 32946.

The time domain simulation is carried out to observe the effect of increased DFIG penetration on the system. The relative rotor angle plots for the

Cases B and C are shown in Figure 6.7 – Figure 6.9. The machines represented in these plots are the dominant machines shown in Figure 6.3.

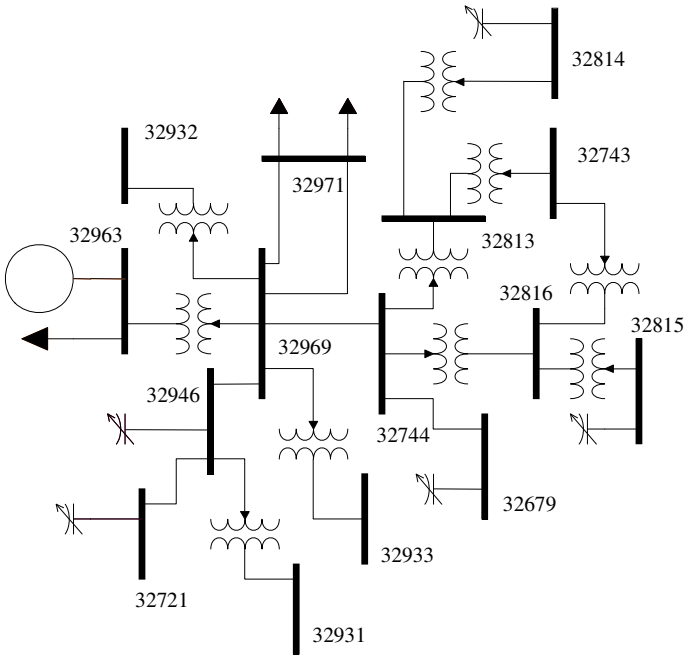

Figure 6.6 Single line diagram showing the bus structure near the generator 32963 with high participation factor

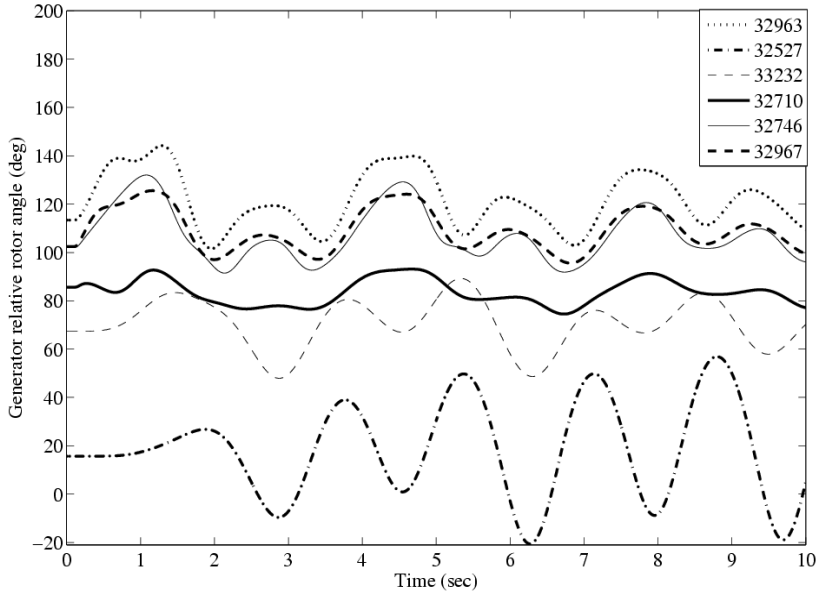

Figure 6.7 Generator relative rotor angle for Case B

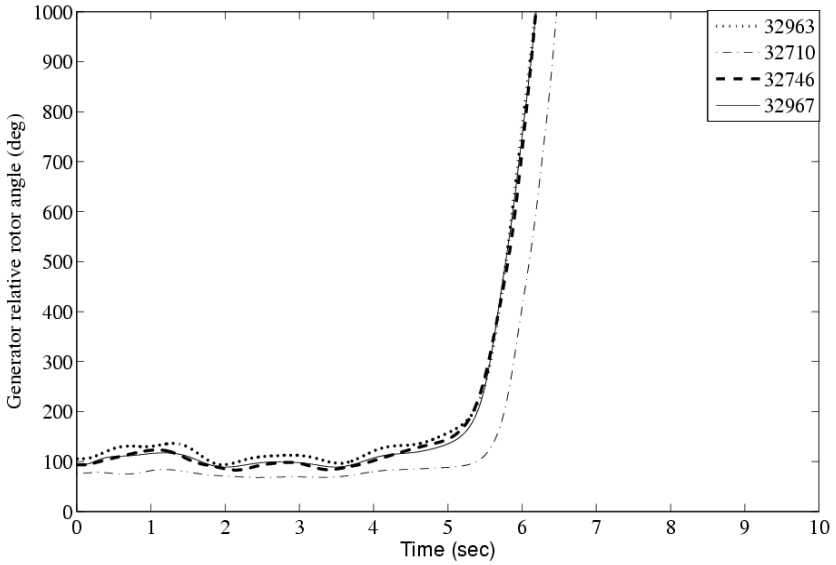

Figure 6.8 Generator relative rotor angle for machines accelerating in Case C

The system is found to be transiently secure in Case B whereas it is found to be transiently insecure in Case C. The machines swinging apart in Case C as a result of the fault can be segregated into accelerating and decelerating groups. The machines that accelerate are shown in Figure 6.8 and the machines that decelerate are shown in Figure 6.9. The result of the disturbance is a large inter area phenomenon as predicted by the small signal analysis shown in Table 6.6.

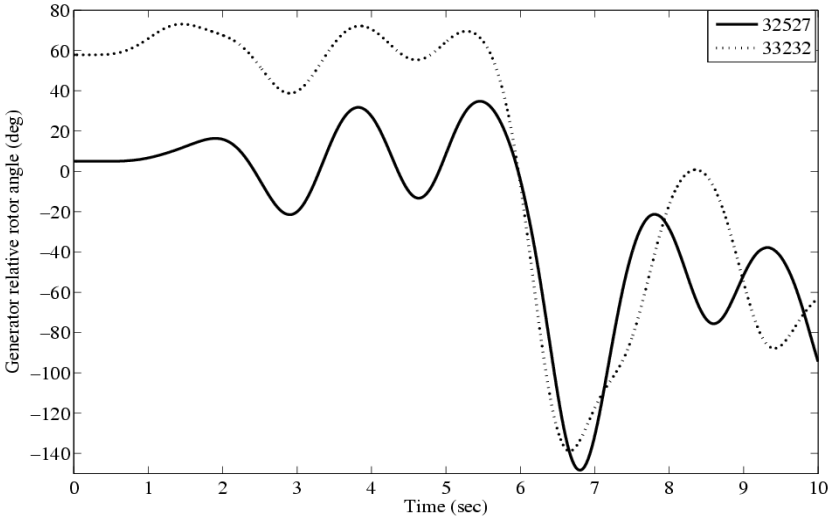

Figure 6.9 Generator relative rotor angle for machines decelerating in Case C

6.3.3. Fault scenario 3 - Beneficial impact on system performance

Following the same procedure adopted for the other two cases for exciting the required mode following a fault, a three phase fault is applied at a 230 kV bus 33270 as shown in Figure 6.4 and is cleared after 6.6 cycles. The fault clearance is followed by clearing the line connecting the buses 33270 and 33290. As the dominant mode considered for small signal analysis corresponds to the speed state of the machines, the generator speeds are observed in time domain.

Figure 6.10 shows the generator speed corresponding to the generator 33216 which is one of the machines participating in the mode as shown in Figure 6.2. The results show that the system is transiently stable for all the four cases and confirms the mode damping ratio results depicted in Table 6.7.

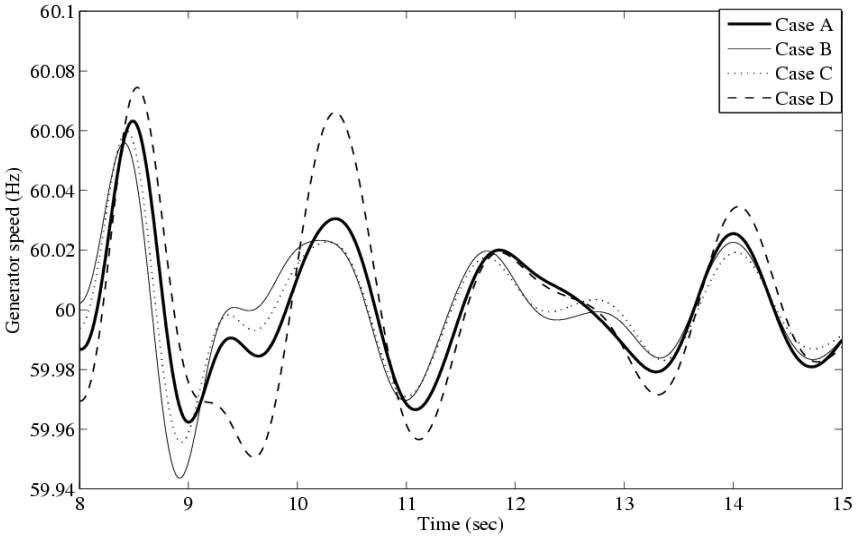

Figure 6.10 Bus 33216 generator speed for Cases A, B, C and D

The damping values in the plots for Cases A-C are very close to each other and accurately reflect the damping ratio results shown in Table 6.7. For Case D the damping is markedly lower and verifies that the higher inertia case will have

the lower damping. The oscillation damping is increased with the increase in DFIG penetration. This fault scenario is thus found to have a beneficial impact with respect to increased wind penetration. The analyses clearly indicate that the results obtained from sensitivity analysis and from eigenvalue analysis are confirmed by exciting the mode in time domain. After having identified the detrimental impact due to reduced inertia, the next step is to supplement DFIG with frequency response capability.

6.4 Frequency support from DFIGs

In order to create load/generation imbalance, 4 generators in the study area, totaling 1950 MW, are disconnected at t = 1 sec. In order to make the frequency drop more apparent in the system, three 345 kV lines are disconnected at the same time. These are the lines transmitting power from generators in the western region to the load centers in the central region of the study area. These changes result in a significant dearth of generation in the load centers and hence result in frequency deviations in a system which is quite robust.

Furthermore, the inertial response of the DFIG is dependent on the initial operating condition, since it is a variable speed machine the stored kinetic energy is different at different operating conditions. At low load some WTG units may be off-line reducing the total wind farm output. This is a difference in comparison with synchronous generation where the inertial response is always constant. In order to quantify maximum inertial response from the DFIG, the present study considers the units to be operating at rated wind speed. The operating condition

considered here is the summer peak load period where the wind farms are providing maximum power output.

The wind farms are connected at the distribution voltage level as mentioned before and spread from the eastern to western part of the system. The distribution voltage level is stepped up and power from all the wind farms is transmitted through a single 161 kV line. This line feeds the load at the central part of the system which had also been fed by the generators being disconnected as mentioned before.

Time domain simulation is carried out for the contingency identified above for the case with and without the supplementary controller.

6.4.1. Influence on power output due to supplementary control

The power output increases for the case with supplementary control compared to the case without it for the first few seconds after the disturbance and again reduces as shown in Figure 6.11.

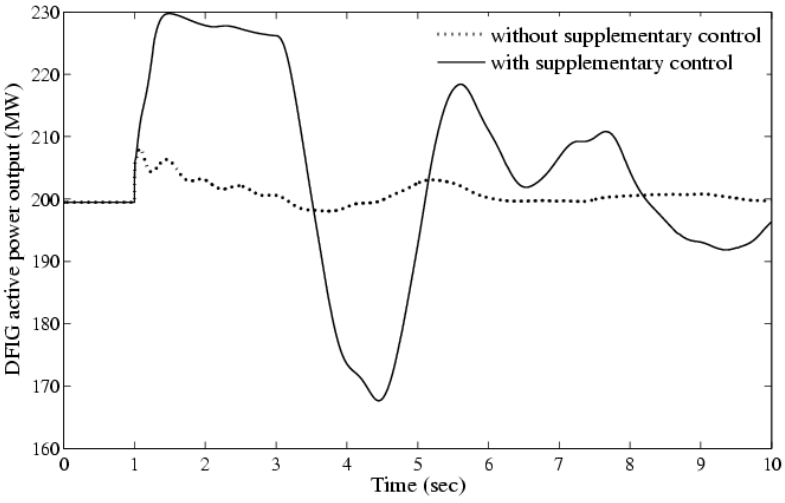

Figure 6.11 DFIG power output at bus 32672 with and without supplementary control

6.4.2. Influence on rotor speed due to supplementary control

It is revealed from Figure 6.12 that this additional output power is possible due to the drop in rotor speed – by extracting kinetic energy from the rotor. The drop in rotor speed as opposed to normal operation shows that DFIG is required to deviate from its optimum speed in order to provide the inertial support. Following inertial response, in order to return to steady state, only a part of aerodynamic power is transmitted to the grid while the rest is used to speed up the turbine back to its optimal speed. Thus, the power output of the DFIG momentarily drops to a value lower than its initial (rated) value immediately after providing inertial support.

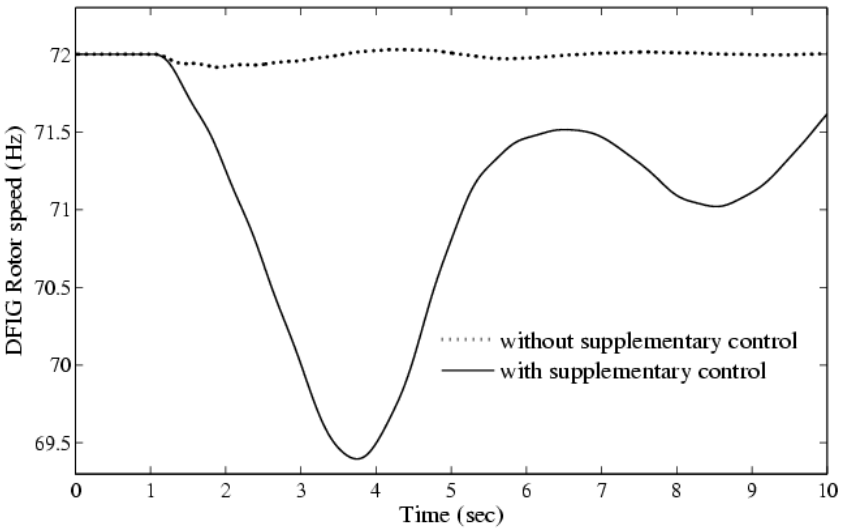

Figure 6.12 Rotor speed of DFIG at bus 32672 with and without supplementary control

6.4.3. Influence on pitch angle controller due to the supplementary control

The action of the pitch angle controller is to limit the mechanical power delivered to the shaft to the equipment rating of 1 p.u. In the case of DFIGs with the newly proposed frequency controller, whenever there is drop in frequency, the

torque set point is increased providing increased power order to the generator. Normally, for power levels above rated, the rotor speed is controlled primarily by the pitch angle controller. However, the electrical dynamics are faster than the dynamics of the pitch angle controller. Hence, the output power of the DFIG will increase by the action of the back-to-back converter acting through the rotor circuit, before the pitch angle controller becomes effective. Given the condition that the DFIG is initially operating at rated power, the increased set point will increase the power output beyond the rated value.

As discussed in section 3.3 , the pitch compensator provides a pitch angle error signal in response to the deviation of output power from the rated value. When the power output increases beyond the rated value (as shown in Figure 6.11), the pitch compensator does not differentiate whether the increase in power output is due to supplementary frequency controller or due to increase in wind speed. The pitch compensator thus acts to increase the pitch angle as shown in Figure 6.13.

The mechanical power extracted from the wind reduces as shown in Figure 6.14 in an attempt to bring the power output to rated value. This drop in mechanical power can be attributed to the reduced value of C_p. The change in shaft speed or pitch angle thus results in a change in captured aerodynamic power as governed by (3.2).

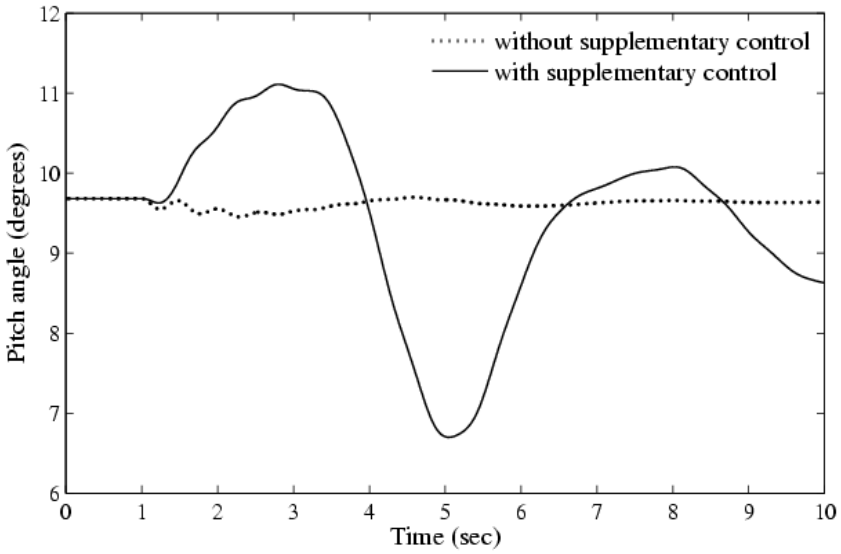

Figure 6.13 Pitch angle of DFIG at bus 32672 with and without supplementary control

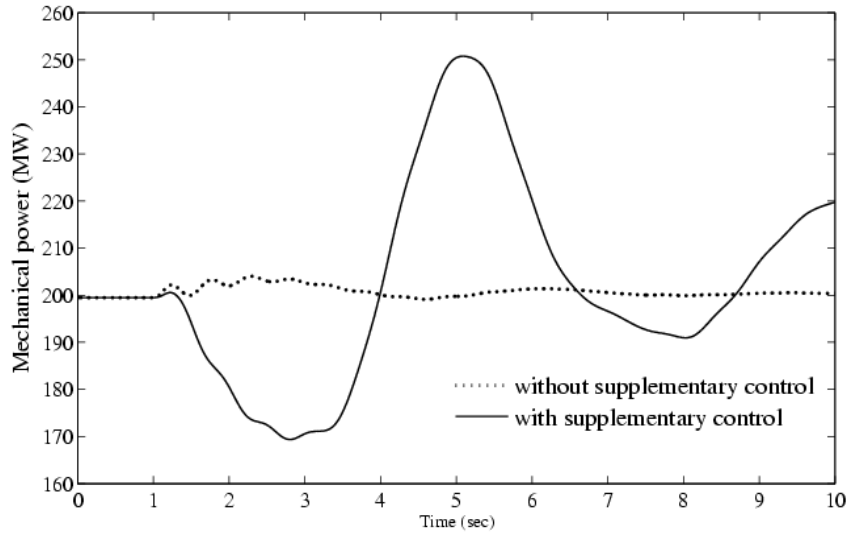

Figure 6.14 Mechanical power of DFIG at bus 32672 with and without supplementary control

6.4.4. Adjustment of pitch compensation and maximum power order

When P_{max} is increased for the chosen controller setting of the supplementary control, the support provided by DFIG also increases. It is to be noted that, the increase in P_{max} for the case without the additional controller does not increase the output power of the DFIG. This validates the fact that implementation of sup-

plementary control effectively serves the purpose of increasing the power output of the DFIG in response to drop in grid frequency.

As the adjustment of both pitch compensation and P_{max} supports the objective of increasing the support from the DFIG in the event of a drop in grid frequency, Figure 6.15 – Figure 6.18 show the plots for the same scenario as depicted in Figure 6.11 – Figure 6.14 but by suitably varying pitch compensator gain so as to aid the supplementary controller and setting the P_{max} = 1.2. It is again emphasized that the actual capability of a DFIG is highly dependent on the rating and design of the equipment. Here the concept, technical theory and results associated with the proposed control strategy are illustrated.

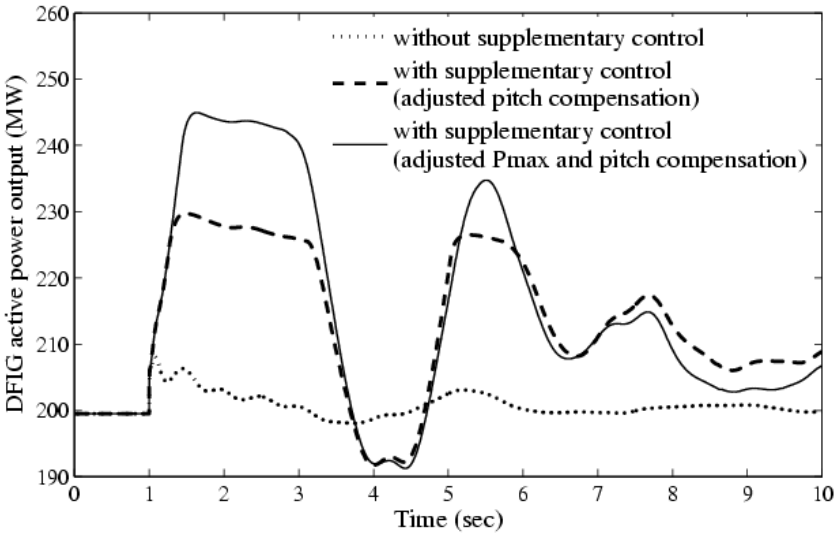

Figure 6.15 Power output of DFIG at bus 32672 with and without supplementary control

It is revealed from Figure 6.16 that the drop in rotor speed is small compared to Figure 6.12, where increase in power is coming solely from the stored

kinetic energy. In the latter case, lesser stored kinetic energy is extracted out of the turbine.

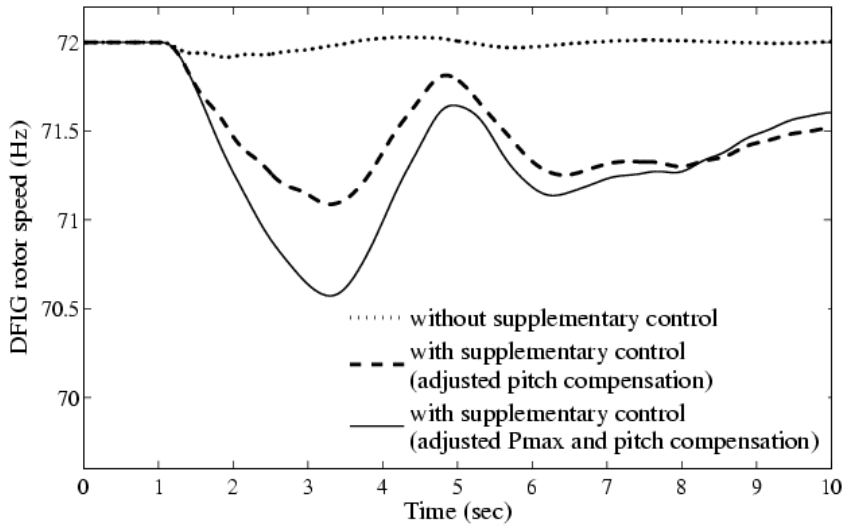

Figure 6.16 Rotor speed of DFIG at bus 32672 with and without supplementary control

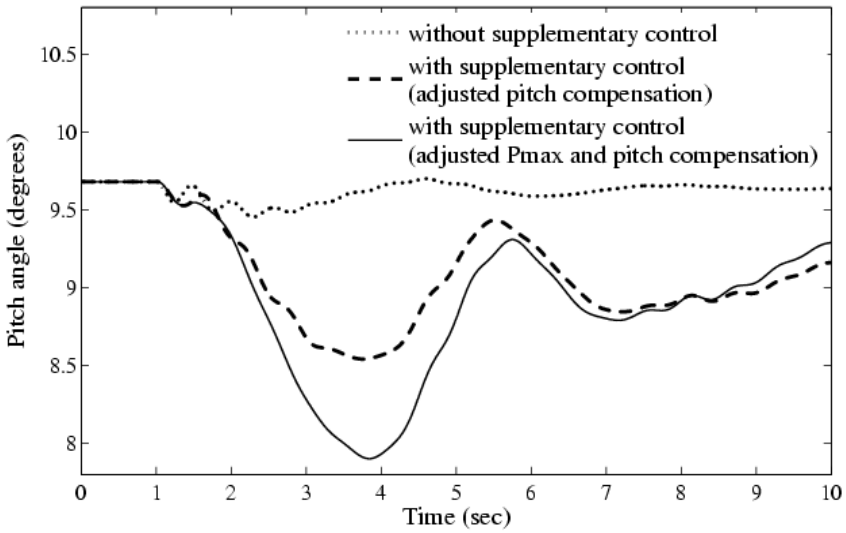

Figure 6.17 Pitch angle of DFIG at bus 32672 with and without supplementary control

It is revealed from Figure 6.11 and Figure 6.15 that the change in pitch compensation gain does not affect peak power but does effect the power nadir

(which occurs after the first peak), the latter being less significant with the changed value of gain. This again supports the statement made earlier – the lesser the speed drop, the smaller the power required to regain the optimal speed and less significant is the power nadir. On the other hand, Figure 6.11 and Figure 6.15 show that with the increase in P_{max}, the peak power increases significantly.

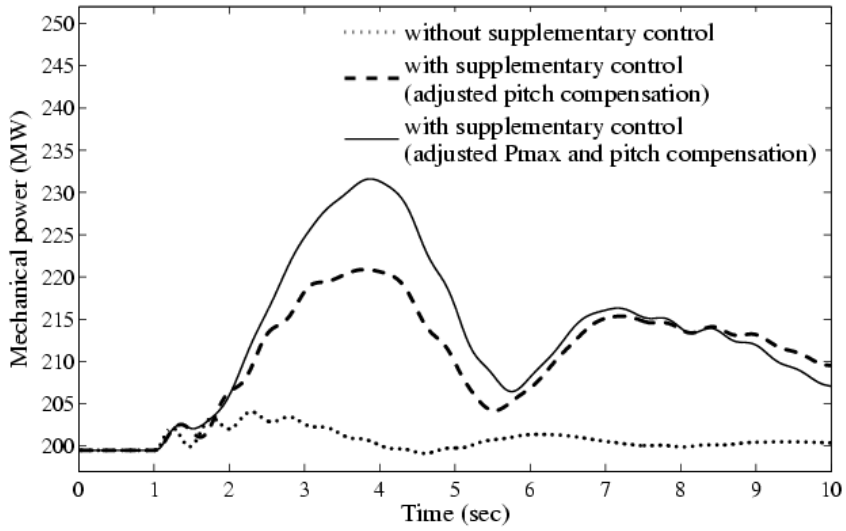

Figure 6.18 Mechanical power of DFIG at bus 32672 with and without supplementary control

After observing the underlying phenomena in the DFIG, frequencies at some of the buses are observed. The buses are selected based on frequency deviation at various voltage levels as well as proximity to wind farms. The bus frequency plots are observed for the case without and with three different cases of supplementary control. These plots are shown in Figure 6.19 – Figure 6.24 for Cases B and C.

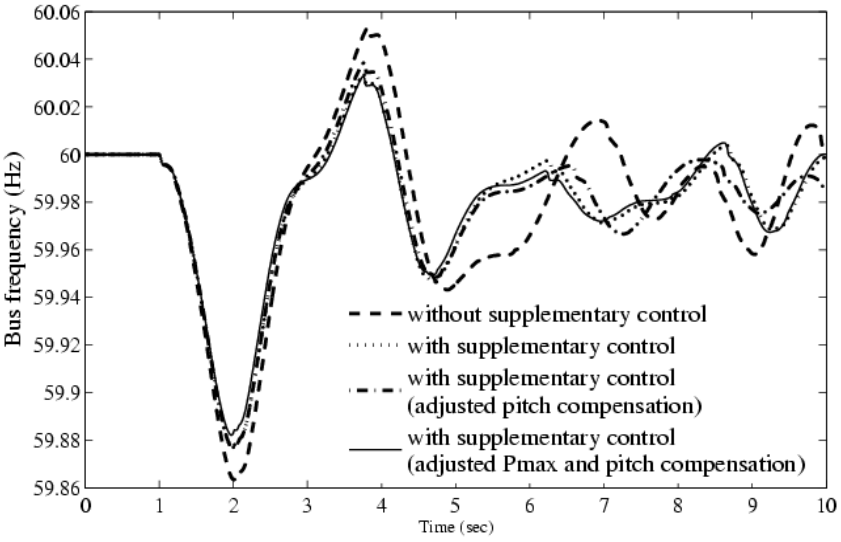

Figure 6.19 Frequency at bus 32969 (345 kV) for Case B

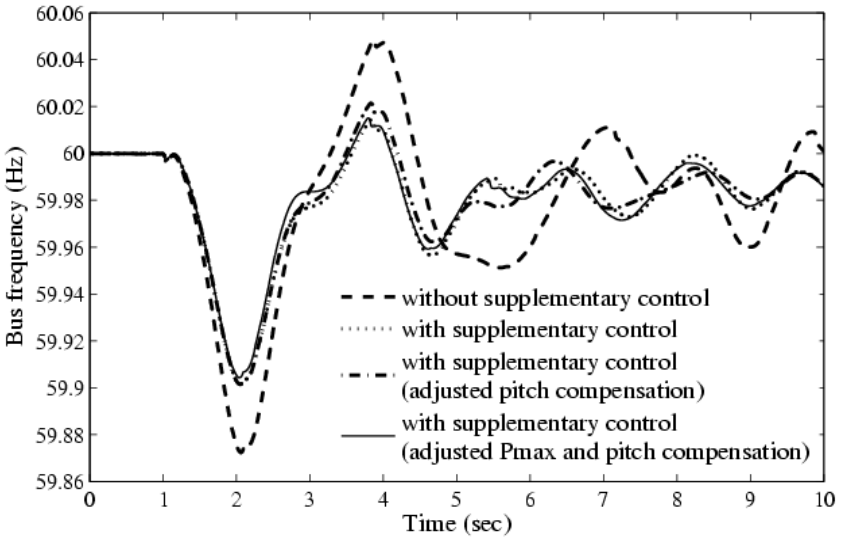

Figure 6.20 Frequency at bus 32969 (345 kV) for Case C

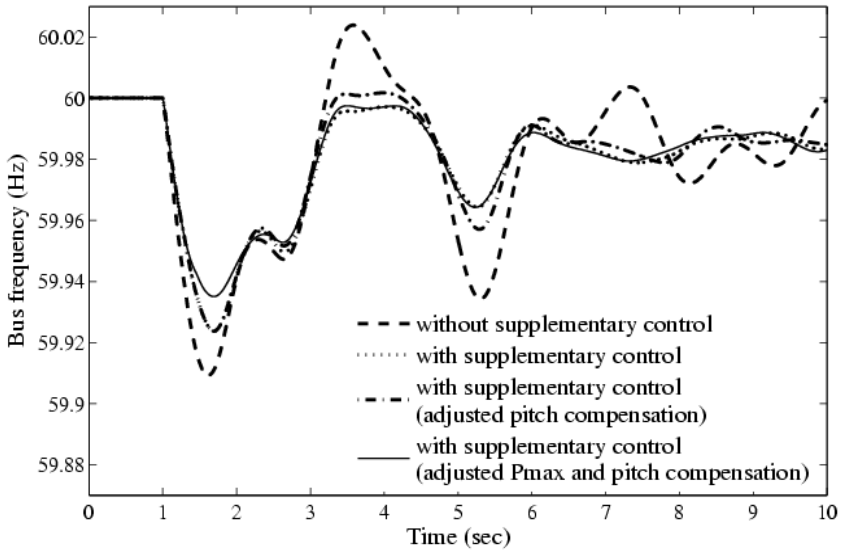

Figure 6.21 Frequency at bus 24222 (161 kV) for Case B

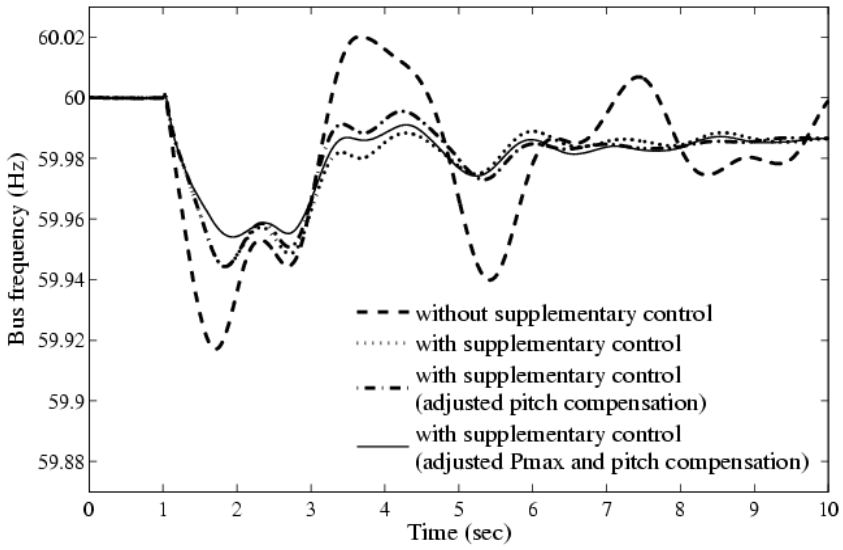

Figure 6.22 Frequency at bus 24222 (161 kV) for Case C

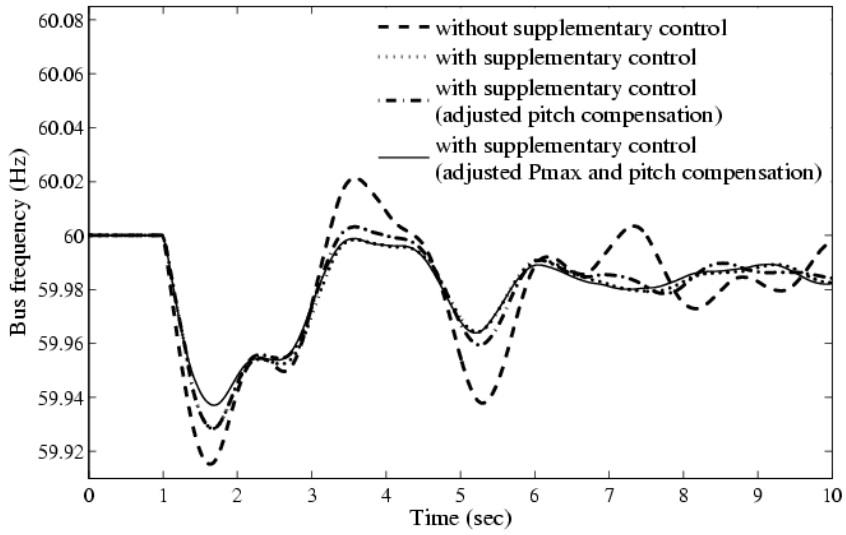

Figure 6.23 Frequency at bus 32729 (69 kV) for Case B

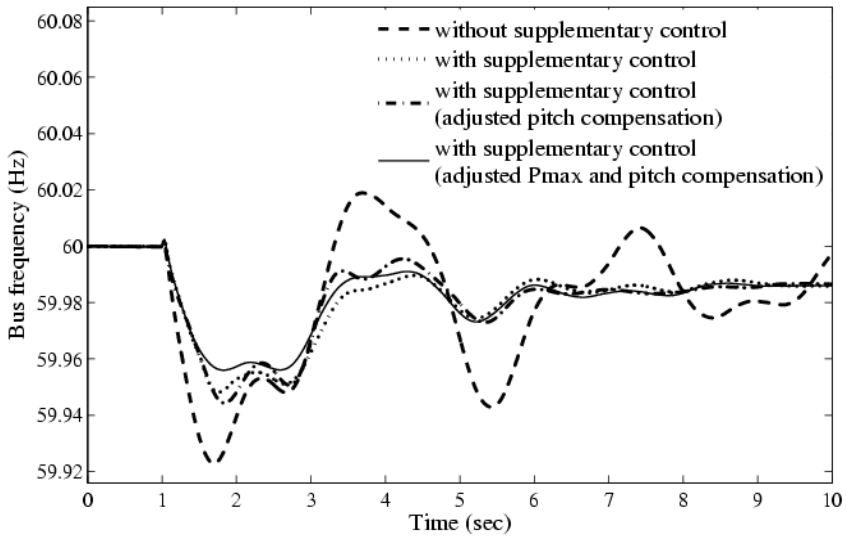

Figure 6.24 Frequency at bus 32729 (69 kV) for Case C

The bus 32969 as shown in Figure 6.19 and Figure 6.20 is the 345 kV bus with the highest frequency deviation while buses 24222 and 32729 are the buses electrically closer to wind farm with high frequency deviation. Apparently, these are the buses leading to the 161kV line where all the wind farm outputs are being

fed. As mentioned in Section 5.3, frequency deviations at the point of interconnection are sensed and used in the supplementary control. Accordingly, bus frequency at 32729 is being sensed and used in the supplementary controller of one of the wind farms.

In order to ensure that the supplementary control does not jeopardize system performance and helps stabilize the system, the simulation is run for 45 s. As shown in Figure 6.25, oscillation in bus frequency is observed for the case without controller. The oscillation inherent to the system for the considered contingency is considerably lowered with the supplementary control.

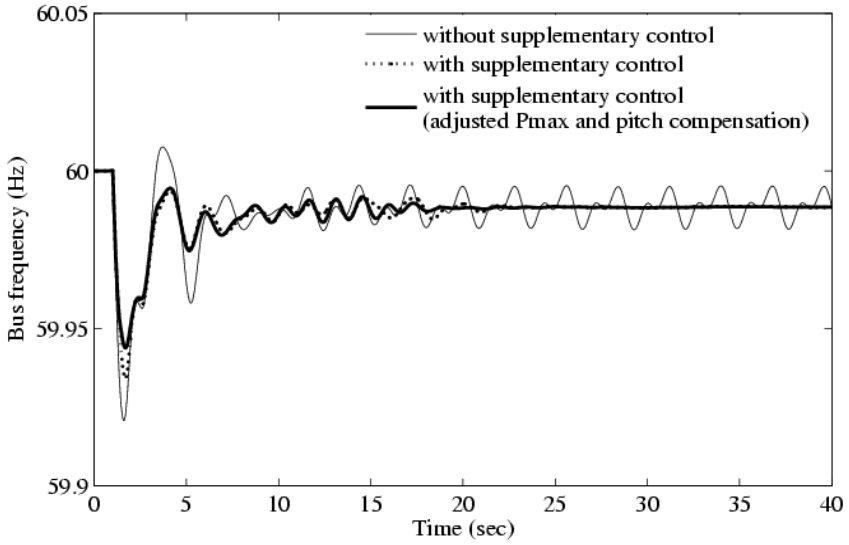

Figure 6.25 Frequency at bus 24222 (161 kV) for Case B

6.4.5. Effect due to wind speed variations

Although wind speed is generally assumed to be constant in transient stability simulation involving wind turbines, simulation has been carried out to incorporate sudden change in wind condition in the form of wind gust and wind

ramp. The idea here is to ensure the validity of the proposed control strategy when the system is subjected to wind disturbance as well as electrical disturbance. The wind speed variations are modeled using two components each of which is added to the initial wind speed to get the actual wind speed. The following two equations, (6.1) and (6.2) represent the wind gust and wind ramp component respectively [56],

$$V_{WG} = \frac{MAXG}{2} \times \left[1 - \cos\left\{ \frac{2\pi\left(t - T_{1g}\right)}{T_g} \right\} \right] \tag{6.1}$$

$$V_{WR} = MAXR \times \left[1 - \frac{\left(t - T_{1r} - T_r\right)}{T_r} \right] \tag{6.2}$$

where, *MAXG* is height of the gust in m/s, T_{1g} is the start time of the gust in seconds, T_g is the length of the gust in seconds, *MAXR* is the height of the ramp in m/s, T_{1r} is the start time of the ramp in seconds, and T_r is the length of the ramp in seconds.

In order to observe the response of the controller for all possible conditions of wind disturbances when the system is subjected to electrical disturbance, separate cases for wind ramp and wind gust are considered. The parameters selected are *MAXG = -3 m/s*, T_{1g} *= 5 s*, T_g *= 6 s*, *MAXR = -3 m/s*, T_{1r} *= 5 s*, and T_r *= 3 s*. The chosen wind ramp parameters result in wind acceleration of -1 m/s^2.

The drop in wind speed is assumed as this leads to drop in rotor speed thus magnifying the effect of drop in rotor speed due to the supplementary control for the contingency considered. As shown in Figure 6.26 the down gust leads to further drop in rotor speed and regains the nominal value after the wind gust is over.

As shown in Figure 6.27 a similar result is observed for the case with wind ramp. It is revealed from the figures that even though the rotor control is subjected to wind gust and wind ramp that magnifies the rotor speed drop due to the contingency, the rotor speed finally stabilizes.

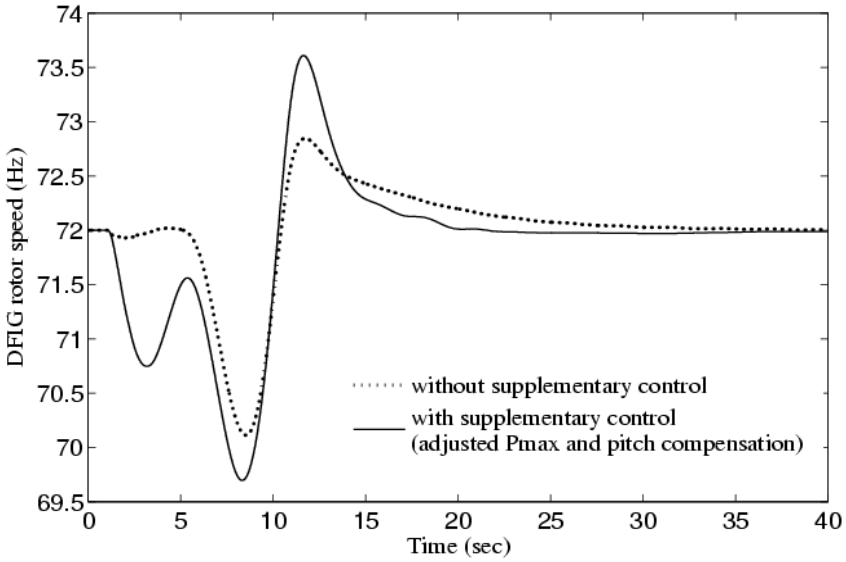

Figure 6.26 Effect of wind gust down on DFIG rotor speed for the cases with and without supplementary control

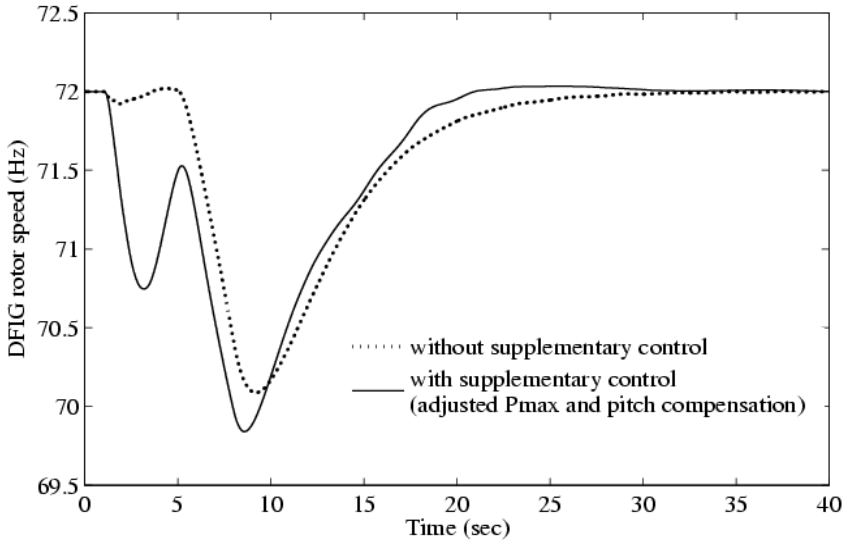

Figure 6.27 Effect of wind ramp down on DFIG rotor speed for the cases with and without supplementary control

Corresponding active power output plots are shown in Figure 6.28 and Figure 6.29. As the wind is ramped down from 14m/s to 11m/s (=14m/s - 3m/s) the power output reduces as shown in Figure 6.29.

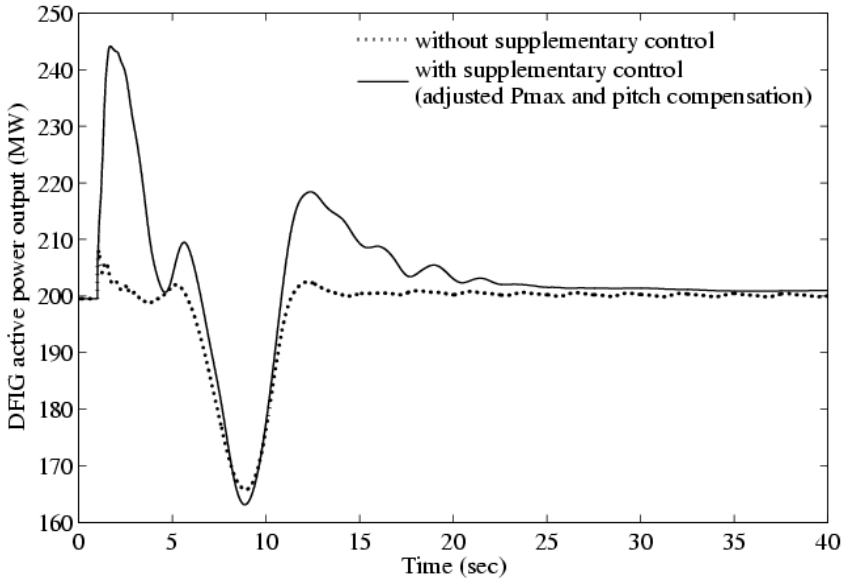

Figure 6.28 Effect of wind gust down on DFIG active power output for the cases with and without supplementary control

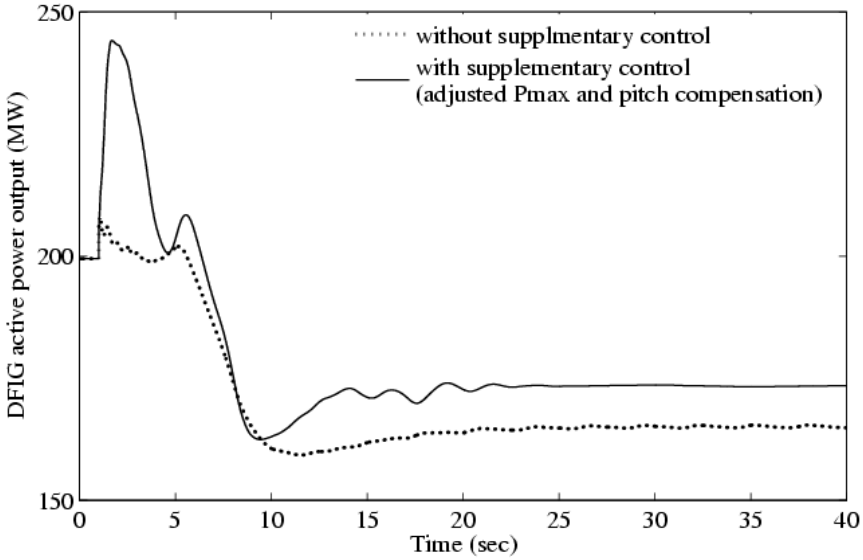

Figure 6.29 Effect of wind ramp down on DFIG active power output for the cases with and without supplementary control

6.4.6. Effect on converter capability

Under all conditions, the current through the converters has to be within the design value, which may otherwise destroy the converters. During all these time domain simulations, active current command demanded by the turbine control model is found to be well within the converter short term active current capability (I_{pmax}) of 1.1 p.u.

6.5 Eigenvalue analysis with supplementary inertia control

The supplementary control also appears to improve the damping in the observed plots. The next step in the analysis is to observe if the implementation of supplementary control has beneficial impact in terms of damping power system oscillations. In order to observe the same, detailed eigenvalue analysis is conducted for Cases B and C in the frequency range of 0.1 Hz to 2 Hz. Table 6.8 and Table 6.9 show the result of eigenvalue analysis corresponding to the mode which has the most improvement in damping with the supplementary control for Cases B and C respectively.

Table 6.8 Dominant mode with beneficial effect due to supplementary control for case B

Case B	Real (1/s)	Imaginary (rad/s)	Frequency (Hz)	Damping ratio (%)	Dominant machine
without supplementary control	-0.0448	3.5351	0.5626	1.27	33232
with supplementary control	-0.058	3.5596	0.5665	1.63	33233
with supplementary control (adjusted Pmax and pitch compensation)	-0.0589	3.5591	0.5664	1.65	33233

This is also the same mode which has a detrimental impact due to reduced inertia with increased penetration of DFIG in the system as demonstrated in Table 6.1. The results demonstrate the improvement in damping with the implementation of supplementary control. The damping is further improved with the adjustment of pitch compensation and P_{max}.

Table 6.9 Dominant mode with beneficial effect due to supplementary control for case C

Case C	Real (1/s)	Imaginary (rad/s)	Frequency (Hz)	Damping ratio (%)	Dominant machine
without supplementary control	-0.0291	3.5072	0.5582	0.83	33233
with supplementary control	-0.0403	3.5261	0.5612	1.14	33233
with supplementary control (adjusted Pmax and pitch compensation)	-0.0409	3.5257	0.5611	1.16	33233

6.6 Eigenvalue analysis with DFIG PSS

Eigenvalue analysis is conducted after implementing DFIG PSS as discussed in section 5.4. Table 6.10 shows the result of eigenvalue analysis corresponding to the mode with detrimental impact as identified in Table 6.1 with the implementation of DFIG PSS. Comparison of Table 6.8 – Table 6.10 for the Cases B and C shows the improvement of damping with the implementation of DFIG PSS. As revealed from Table 6.8 – Table 6.10, between the two control mechanisms, better damping performance is obtained with the implementation of DFIG PSS.

Table 6.10 Result summary for Case B and Case C with DFIG PSS for the dominant mode with detrimental effect on damping

Case	Real (1/s)	Imaginary (rad/s)	Frequency (Hz)	Damping ratio (%)	Dominant machine
B	-0.0593	3.5157	0.5595	1.69	33232
C	-0.0413	3.4908	0.5556	1.18	33232

6.7 Eigenvalue analysis with both controllers

The next step was to observe what effect implementation of both controllers has on damping of the critical mode. In order to accomplish the same, DFIG is equipped with both inertia controller and DFIG PSS. Corresponding eigenvalue analysis result is shown in Table 6.11. Comparative study of the results obtained reveal that the damping performance is improved with the implementation of both the controllers.

Table 6.11 Result summary for Case B and Case C with DFIG PSS and inertia controller for the dominant mode with detrimental effect on damping

Case	Real (1/s)	Imaginary (rad/s)	Frequency (Hz)	Damping ratio (%)	Dominant machine
B	-0.0651	3.5206	0.5603	1.85	33232
C	-0.0470	3.4959	0.5564	1.35	33232

6.8 Transient stability analysis with supplementary inertia control

In conducting the transient stability analysis the same scenario and contingency as discussed in section 6.3.1 is considered. As shown in Figure 6.30 and Figure 6.31 the damping improvement is also observed in time domain with the implementation of supplementary inertia control.

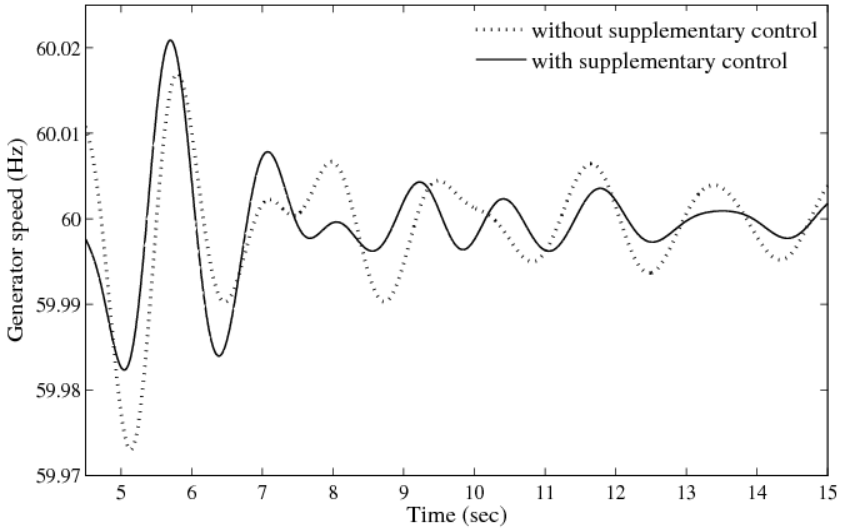

Figure 6.30 Generator speed for the bus 33232 for the Case B

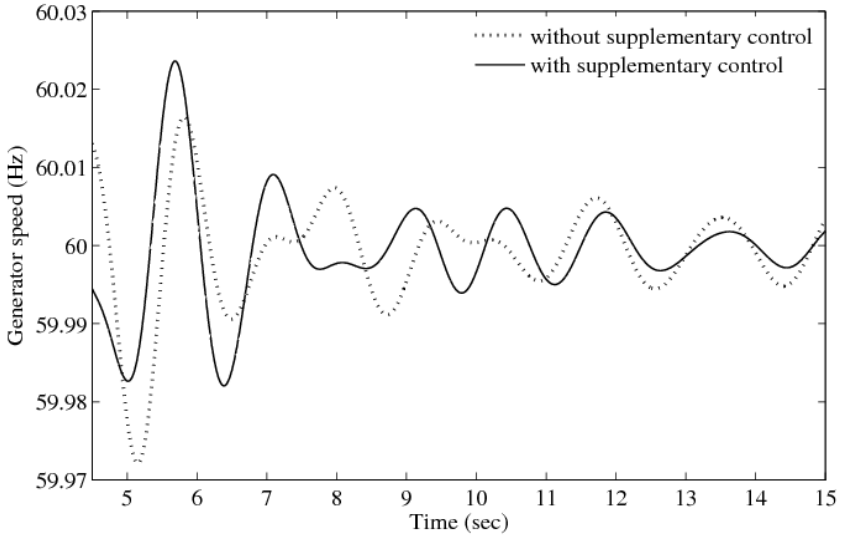

Figure 6.31 Generator speed for the bus 33232 for the Case C

As the dominant mode considered for small signal analysis corresponds to the speed state of the machines, the generator speed corresponding to the dominant machine 33232 is observed in time domain. No difference in damping is observed between the cases with and without adjusting P_{max} and pitch

compensation. Also apparent from Table 6.8 and Table 6.9, adjustment of P_{max} and pitch compensation does not make significant improvement in damping.

CHAPTER 7

CONCLUSIONS AND FUTURE WORK

7.1 Conclusions

In this dissertation, the impact of increased penetration of DFIG based WTGs on small signal stability and transient stability is examined for a realistic large system. The work is further extended to develop the control strategies to mitigate the impact of reduced inertia due to increased penetration of DFIGs on the system.

In order to examine the impact on small signal stability, a systematic approach to pin point the impact of increased penetration of DFIGs on electromechanical modes of oscillation using eigenvalue sensitivity with respect to inertia is developed. The sensitivity analysis identifies electromechanical modes of oscillations that are detrimentally and beneficially impacted by increased DFIG penetration. The results of the sensitivity analysis are then confirmed using exact eigenvalue analysis performed by including the DFIGs in the base case and in the increased wind penetration case.

Each of the critical modes obtained in the small signal stability study is scrutinized in time domain. The objective of transient stability analysis is to examine if the modes identified in the small signal stability analysis can be excited by the large disturbance. The modes observed in small signal analysis are excited by placing specific faults at buses close to the generators having the largest participation factors in the oscillatory modes identified.

For the system operating conditions considered, the analysis conducted indicates that it is possible to identify a certain inter-area mode which is detrimentally affected by the increased DFIG penetration. Moreover, using the concept of participation factors, the specific mode can be excited in time domain.

The system is found to have both beneficial and detrimental impact with the increased penetration of DFIG. Both these situations observed by sensitivity analysis for small signal stability are also observed in nonlinear time domain analysis by considering corresponding fault scenarios in time domain.

The sensitivity of the real part of the eigenvalue with respect to inertia evaluated for a system where the DFIGs at their planned insertion points in the network are replaced by equivalent round rotor synchronous machines provides a good metric to evaluate the impact due to increased DFIG penetration on system dynamic performance. The eigenvalue sensitivity analysis together with the detailed eigenvalue analysis is also substantiated by the results obtained from time domain simulation.

The control strategies are developed to mitigate the impact of reduced inertia due to DFIGs in the large power system. The strategy effectively serves the purpose of improving the frequency deviation following a disturbance. The adjustment in pitch compensation gain and P_{max} is found to support the objective of increasing the support from the DFIGs in the event of deviation in grid frequency. Significantly better improvement in frequency is observed as the value of P_{max} is increased. The simulations carried out ensure the power and current demanded by

the controller to be within the converter design value. However, this is limited by operational and design constraints of the actual equipment. Hence, this must be considered by equipment manufacturers and some design modifications might be required to raise the value of P_{max} so as to achieve even better frequency response capability.

The proposed control mechanism is also validated against sudden wind gusts and wind ramps. Although the wind changes magnify the drop in rotor speed due to the supplementary control for the contingency considered, the rotor speed finally stabilizes.

The implementation of the supplementary control block is found to have beneficial impact in terms of damping power system oscillations. The damping improvement for the same mode observed in the time domain is found to support the result obtained from eigenvalue analysis.

A control mechanism for a DFIG similar to the PSS in case of synchronous machines is proposed so as to damp low frequency inter-area modes of oscillation. Effectively, DFIG PSS consists of both the active as well as reactive power modulated components.

Although supplementary inertia control as well as DFIG PSS serves the purpose of improving the damping of the mode with detrimental impact, among the two, better performance is obtained with the implementation of DFIG PSS. Even better damping performance is observed when DFIG is equipped with both supplementary controllers.

7.2 Future work and recommendation

In the present work supplementary control gain is designed based on the MVA ratings of the DFIG wind farms and maximum deviation in the grid frequency at the point of interconnection among all the wind farms. This work can be extended by implementing the adaptive control mechanism which can precisely capture the deviation in the grid frequency at the point of interconnection of the wind farm.

The contribution of wind turbines in response to frequency excursion in the grid cannot be sustained indefinitely due to limited stored kinetic energy. In order to eliminate the steady state frequency error, unless the wind turbines are initially operating at de-loaded conditions, conventional synchronous machines equipped with governors must provide secondary response and bring the frequency error to zero.

REFERENCES

[1] S. Heier, *Grid Integration of Wind Energy Conversion Systems*, Chichester, U.K.: John Wiley & Sons Ltd., 2006.

[2] Global Wind Energy Council (GWEC), "Global wind 2009 report," Available online: http://www.gwec.net/fileadmin/documents/Publications/Global_Wind_2007_report/GWEC_Global_Wind_2009_Report_LOWRES_15th.%20Apr..pdf.

[3] N. Miller, Z. Ye, "Report on distributed generation penetration study," National Renewable Energy Laboratory, CO, Tech Rep. August 2003. Available online: www.nrel.gov/docs/fy03osti/34715.pdf

[4] P. M. Anderson and A. A. Fouad, *Power System Control and Stability*, N.J.: John Wiley & Sons, Inc., 2002.

[5] J. J. Grainger and W. D. Stevenson, *Power System Analysis*, New York: McGraw-Hill, 1994.

[6] H. Knudsen and J. N. Nielsen, "Introduction to the modeling of wind turbines," in *Wind Power in Power Systems*, T. Ackermann, Ed. Chicester, U.K.: Wiley, 2005, pp. 525-585.

[7] J. G. Slootweg, S. W. H. de Haan, H. Polinder and W. L. Kling, "Modeling wind turbines in power system dynamics simulations," in *Proc. 2001 IEEE Power Engineering Society Summer Meeting*, vol. 1, pp. 22-26.

[8] M. Poller and S. Achilles, "Aggregated wind park models for analyzing power system dynamics," in *Proc. 4th International Workshop on Large-Scale Integration of Wind Power and Transmission Networks for Offshore Wind Farms*, 2003.

[9] P.W. Carlin, A.S. Laxson and E.B. Muljadi "The history and state of the art of variable-speed wind turbine technology," Tech. Rep., National Renewable Energy Laboratory, 2001. Available online: http://www.nrel.gov/docs/fy01osti/28607.pdf

[10] L. Holdsworth, X.G. Wu, J.B. Ekanayake and N. Jenkins, "Comparison of fixed speed and doubly-fed induction wind turbines during power system disturbances," in *Proc. 2003 IEE Generation, Transmission and Distribution,* pp. 343-352.

[11] J. Usaola and P. Ledesma, "Dynamic incidence of wind turbines in networks with high wind penetration," in *Proc. 2001 IEEE Power Engineering Society Summer Meeting*, pp. 755-760.

[12] M. A. Poller, "Doubly-fed induction machine models for stability assessment of wind farms," in *Proc. 2003 IEEE Bologna PowerTech Conference*.

[13] N. Jenkins, R. Allan, P. Crossley, D. Kirschen and G. Strbac, *Embedded Generation*, IEE Power and Energy Series 31, U.K.: TJ International Ltd., 2000.

[14] C. Eping, J. Stenzel, M. Poller, and H. Muller, "Impact of large scale wind power on power system stability," presented at *5th International Workshop on Large-Scale Integration of Wind Power and Transmission Networks for Offshore Wind Farms*, 2005.

[15] A. Causebrook and B. Fox, "Modernising grid codes to accommodate diverse generation technologies, especially modern wind farms," *Wind Engineering*, vol. 28, no. 1, pp. 75-86, 2004.

[16] F. M. Hughes, O. A. Lara, N. Jenkins and G. Strbac, "Control of DFIG – based wind generation for power network support," *IEEE Trans. Power Systems*, vol. 20, no. 4, pp. 1958-1966, November 2005.

[17] L. R. C. Chien, C. M. Hung and Y. C. Yin, "Dynamic reserve allocation for system contingency by DFIG wind farms," *IEEE Trans. Power Systems*, vol. 23, no. 2, pp. 729-736, May 2008.

[18] J. F. Conroy and R. Watson, "Frequency response capability of full converter wind turbine generators in comparison to conventional generation," *IEEE Trans. Power Systems*, vol. 23, no. 2, pp. 601-612, May 2008.

[19] N. R. Ullah, T. Thiringer and D. Karlsson, "Temporary primary frequency control support by variable speed wind turbines – potential and applications," *IEEE Trans. Power Systems*, vol. 23, no. 2, pp. 601-612, May 2008.

[20] J. B. Ekanayake, L. Holdsworth, X. Wu and N. Jenkins, "Dynamic modeling of doubly fed induction generator wind turbines," *IEEE Trans. Power Systems*, vol. 18, no. 2, pp. 803-809, May 2003.

[21] M. Kayikci and J. V. Milanovic, "Assessing transient response of DFIG – based wind plants – the influence of model simplifications and parameters," *IEEE Trans. Power Systems*, vol. 23, no. 2, pp. 545-554, May 2008.

[22] M. V. A. Nunes, J. A. P. Lopes, H. H. Zurn, U. H. Bezerra, and R. G. Almeida "Influence of the variable-speed wind generators in transient stability margin of the conventional generators integrated in electrical grids," *IEEE Trans. Energy Conversion*, vol. 19, no. 4, pp. 692-701, December 2004.

[23] E. Muljadi, C. P. Butterfield, B. Parsons and A. Ellis, "Effect of variable speed wind turbine generator on stability of a weak grid," *IEEE Trans. Power Systems*, vol. 22, no. 1, pp. 29-35, March 2008.

[24] T. Sun, Z. Chen and F. Blaabjerg, "Transient stability of DFIG wind turbines at an external short-circuit fault," *Wind Energy*, vol. 8, pp. 345-360, August 2005.

[25] N. R. Ullah and T. Thiringer, "Effect of operational modes of a wind farm on the transient stability of nearby generators and on power oscillations: a Nordic grid study," *Wind Energy*, vol. 11, pp. 63-73, September 2007.

[26] L. Rouco, "Eigenvalue-based methods for analysis and control of power system oscillations," in *Proc. 1998 IEE Colloquium on Power Dynamics Stabilization*, pp. 1-6.

[27] J. J. Sanchez Gasca, N. W. Miller and W. W. Price, "A modal analysis of a two-area system with significant wind power penetration," in *Proc. 2004 IEEE PES Power Systems Conference and Exposition*, pp. 1148-1152.

[28] J. G. Slootweg and W. L. Kling, "The impact of large scale wind power generation on power system oscillations," *Electric Power Systems Research*, vol. 67, no. 1, pp. 9-20, October 2003.

[29] R. D. Fernandez, R. J. Mantz and P. E. Battaiotto, "Impact of wind farms on power system - an eigenvalue analysis approach," *Renewable Energy*, vol. 32, no. 10, pp. 1676-1688, August 2007.

[30] F. Xu, X. P. Zhang, K. Godfrey and P. Ju, "Modeling and control of wind turbine with doubly fed induction generator," in *2006 Proc. IEEE PES Power Systems Conference and Exposition*, pp. 1404-1409.

[31] F. Xu, X. P. Zhang, K. Godfrey and P. Ju, "Small signal stability analysis and optimal control of a wind turbine with doubly fed induction generator" in *Proc. 2007 IET Generation, Transmission & Distribution*, pp. 751-760.

[32] A. Mendonca and J. A. P. Lopes, "Impact of large scale wind power integration on small signal stability," in *Proc. 2005 International Conference on Future Power Systems,* pp. 1-5.

[33] F. Mei, B. Pal, "Modal analysis of grid connected doubly fed induction generators," *IEEE Trans. Energy Conversion*, vol. 22, no. 3, pp. 728-736, September 2007.

[34] J. Ekanayake and N. Jenkins, "Comparison of the response of doubly fed and fixed-speed induction generator wind turbines to changes in network frequency," *IEEE Trans. Energy Conversion*, vol. 19, no. 4, December 2004.

[35] G. Lalor, A. Mullane and M. O. Malley, "Frequency control and wind turbine technologies," *IEEE Trans. Power Systems*, vol. 20, no. 4, pp. 1905-1912, November 2005.

[36] J. Morren, S. W. H. Haan, W. L. Kling and J. A. Ferreira, "Wind turbines emulating inertia and supporting primary frequency control," *IEEE Trans. Power Systems*, vol. 21, no. 1, pp. 433-434, February 2006.

[37] R. G. Almeida and J. A. P. Lopes, "Participation of doubly fed induction wind generators in system frequency regulation," *IEEE Trans. Power Systems*, vol. 22, no. 3, pp. 944-950, August 2007.

[38] G. Ramtharan, J. B. Ekanayake and N. Jenkins, "Frequency support from doubly fed induction generator wind turbines," *IET Renew. Power Generation*, vol. 1, no. 1, pp. 3-9, March 2007.

[39] N. R. Ullah, T. Thiringer and D. Karlsson, "Temporary primary frequency control support by variable speed wind turbines – potential and applications," *IEEE Trans. Power Systems*, vol. 23, no. 2, pp. 601-612, May 2008.

[40] N. Miller, K. Clark, R. Delmerico and M. Cardinal, "Windinertia^{TM}: Inertial response option for GE wind turbine generators," presented at *2009 IEEE Power Engineering Society General Meeting*.

[41] P. K. Keung, P. Li, H. Banakar and B. T. Ooi, "Kinetic energy of wind-turbine generators for system frequency support," *IEEE Trans. Power Systems*, vol. 24, no. 1, pp. 279-287, February 2009.

[42] J. M. Mauricio, A. Marano, A. G. Exposito and J. L. M. Ramos, "Frequency regulation contribution through variable-speed wind energy conversion systems," *IEEE Trans. Power Systems*, vol. 24, no. 1, pp. 173-180, February 2009.

[43] F. M. Hughes, O. A. Lara, N. Jenkins, G. Strbac, "A power system stabilizer for DFIG – based wind generation," *IEEE Trans. Power systems*, vol. 21, no. 2, May 2006.

[44] G. Tsourakis, B. M. Nomikos, C. D. Vournas, "Contribution of doubly fed wind generators to oscillation damping," *IEEE Trans. Energy Conversion*, vol. 24, no. 3, September 2009.

[45] A. Mendonca and J. A. P. Lopes, "Simultaneous tuning of power system stabilizers installed in DFIG – based wind generation," in *Proc. 2007 IEEE Lausanne Power Tech*., pp. 219 - 224.

[46] N. W. Miller, W. W. Price and J. J. Sanchez-Gasca, "Modeling of GE wind turbine-generators for grid studies," General Electric International, Inc., Schenectady, NY, Tech. Rep. version 3.4b, March 2005.

[47] CIGRE Technical Brochure "Modeling and dynamic behavior of wind generation as it relates to power system control and dynamic performance," Working Group 01, Advisory Group 6, Study Committee C4, Draft Report, August 2006.

[48] Powertech Labs Inc., DSA Tools model manual, Version 7.1.

[49] P. Kundur, J. Paserba, V. Ajjarapu, G. Andersson, A. Bose, C. Canizares, N. Hatziargyriou, D. Hill, A. Stankovic, C. Taylor, T. V. Custem and V. Vittal, "Definition and classification of power system stability," *IEEE Trans. Power Systems*, vol. 19, no. 2, pp. 1387-1401, May 2004.

[50] P. Kundur, *Power System Stability and Control*, New York: McGraw Hill Inc., 1994.

[51] D. K. Faddeev and V. N. Faddeeva, *Computational Methods of Linear Algebra*, San Francisco and London: W. H. Freeman and Company, 1963.

[52] J.E. Van Ness, J.M. Boyle, and F.P. Imad, "Sensitivities of large, multiple – loop control systems", *IEEE Trans. Automatic Control*, vol. 10, no. 3, pp. 308-315, July 1965.

[53] T. Smed, "Feasible eigenvalue sensitivity for large power systems," *IEEE Trans. Power Systems*, vol. 8, no. 2, pp. 555-561, May 1993.

[54] J. Ma, Z. Y. Dong and P. Zhang, "Eigenvalue sensitivity analysis for dynamic power system," in *Proc. 2006 International Conference on Power System Technology*, pp. 1-7.

[55] T. K. Kiong, W. Q. Guo, H. C. Chieh, T. J. Hagglund, *Advances in PID control*, London: Springer – Verlag London Limited, 1999.

[56] P. M. Anderson and A. Bose, "Stability simulation of wind turbine systems," *IEEE Trans. Power Apparatus and System*, vol. PAS-102, no. 12, pp. 3791-3795, December 1983.